Inverse Problems and Imaging
Vol. 18, No. 4, August 2024, pp. 993-1023
doi:10.3934/ipi.2024004

SHOWER CURTAIN EFFECT AND SOURCE IMAGING

Josselin Garnier[1] and Knut Sølna[2]

[1]Centre de Mathématiques Appliquées, Ecole Polytechnique,
Institut Polytechnique de Paris, 91120 Palaiseau, France

[2]Department of Mathematics, University of California, Irvine CA 92697

(Communicated by Kui Ren)

Abstract. The shower curtain effect is commonly described as being able to see a person behind a shower curtain better than that person can see us. This asymmetric phenomenon has been observed in numerical simulations in various propagation models and in optics experiments. Here we present an analysis in the paraxial regime to give a novel characterization of the mechanism behind this effect and we discuss applications to imaging. The paraxial regime is for instance appropriate to model the propagation of a laser beam in a turbulent atmosphere. The theory that we present has also applications to tissue imaging. We consider two different measurement and imaging setups (matched field imaging and optical imaging) to clarify the shower curtain mechanism. We give a quantitative description of how the placement of the shower curtain, modeled as a randomly heterogeneous section, affects the optical imaging resolution. We moreover analyze the signal-to-noise ratio of the image. The analysis involves the study of multifrequency fourth-order moments associated with the Itô-Schrödinger equation and reveals that broadband sources are necessary to ensure statistical stability and high signal-to-noise ratio.

1. **Introduction.** An interesting phenomenon in optics is that it is possible to see a person behind a shower curtain better than that person can see us. This effect has been referred to as the shower curtain effect [12]. Here we address the challenge of giving a precise mathematical description of this phenomenon. In addition to identify what governs the effect we discuss how imaging algorithms can be designed and analyzed when the objective is to image a source hidden behind the 'shower curtain'. We view the shower curtain as a complex section of finite width localized between the detector and the source and we model this complex section as a random medium.

The central aspect of the shower curtain effect is that, in addition to the scattering properties of the random medium, the relative location of the random medium section between the source and the detector also affects the image quality for standard imaging devices (such as the human eye) [4, 13, 14]. The motivation in [13] is to analyze how atmospheric clouds affect imaging performance and in particular the role of the relative position of the clouds. Numerical illustrations based on a radiative transfer model are presented in [13]. In [12] the authors consider the role of the relative position of a complex section in the situation with time reversal of waves. In

2020 *Mathematics Subject Classification.* 60H15, 35R60, 74J20.

Key words and phrases. Optics, waves in random media, shower curtain effect, imaging, multiple scattering, paraxial approximation.

this case a source is beaming and the propagated field is recorded on a time-reversal mirror, that is, the complex field is recorded, time reversed, and re-emitted. The re-emitted field then refocuses at the original source location. The authors illustrate numerically a shower curtain effect in this setting in that the refocusing is all the better as the complex section is closer to the source. In their study the authors use a paraxial modeling framework and a Gaussian approximation for the statistics of the wave field to enable computation of fourth-order moments. Recently the shower curtain effect has also been considered in the context of speckle imaging [5, 21, 15]. In these papers the autocorrelation of a mask function or object to be imaged is derived from wave speckle patterns and a phase retrieval algorithm is used to retrieve the mask function. In speckle imaging a shower curtain effect also affects the imaging performance. We remark that speckle imaging is analyzed in [10] in the wave regime we consider here and the analytic framework set forth there can be extended to the shower curtain setting considered here. Aspects of the shower curtain effect from the point of view of active imaging configurations and illumination aspects are discussed in [20]. In [18, 19] an active imaging configuration in Optical Coherence Tomography is considered. In these papers it is argued that the system performance can be understood and enhanced partly from the point of view of the shower curtain effect. Here we consider the passive imaging case with a source to be imaged and we give a precise characterization of how the properties of the random section and its relative location affect the performance of source imaging through the section in the white-noise paraxial regime. Central to our discussion is an analysis of the signal-to-noise ratio for the imaging algorithm. We show that the signal-to-noise ratio may be very low depending on the imaging modality, however, that the use of broadband (multifrequency) signals may enable imaging. This characterization derives from recent results for multifrequency fourth-order moments for the waves in random media.

The outline of the paper is as follows. In section 2 we summarize the main results. We consider wave propagation in the white-noise paraxial regime and present this regime in section 3. The two imaging modalities that we consider, matched field imaging and optical imaging, are presented in section 5 in the case of full aperture. The case of imaging with partial aperture is analyzed in section 6. One main focus of the analysis is to characterize imaging resolution and how it relates to the shower curtain effect. However, imaging with high resolution is of little use if the image has low signal-to-noise ratio and in section 7 we discuss how one can obtain high signal-to-noise ratio in the optical set-up by broadband imaging.

2. **Summary of results.** We will study two imaging modalities: matched field imaging and optical imaging.

Consider first the matched field imaging set-up illustrated in Figure 1. Here the source is located to the left in the plane $z = 0$ and the wave field propagates through a random section located in the range interval $z \in (z_{\rm a}, z_{\rm b})$. This random section models the shower curtain. The transmitted complex field is measured in the detector plane $z = z_1$ beyond the shower curtain. Our objective is to image the transversal support function of the time-harmonic source. The source spatial function is denoted by $f(\boldsymbol{x})$ for $\boldsymbol{x}$ the lateral spatial coordinates. We consider the paraxial white-noise regime described in section 3 modeling high-frequency beam waves in a random medium. This description allows us to analyze the image and its statistical moments, with the moments being computed with respect to the randomness in the complex section.

In the matched field imaging set-up the transmitted complex field is recorded and the matched field image is obtained by matching or correlating it with the point source response:

$$\mathcal{U}(\boldsymbol{x}) = \int_{\mathbb{R}^2} \hat{v}(\boldsymbol{y}, z_1)\overline{\hat{G}(\boldsymbol{x}, \boldsymbol{y}, z_1)} \exp\Big(- \frac{|\boldsymbol{y}|^2}{2D^2}\Big) \mathrm{d}\boldsymbol{y}, \tag{1}$$

where $\hat{v}$ the transmitted complex time-harmonic wave field (measured by the detector) and $\hat{G}(\boldsymbol{x}, \boldsymbol{y}, z)$ the time-harmonic Green's function. That is, $\hat{G}$ is the synthetic field in a homogeneous medium with constant speed of propagation c_o when recorded at $(\boldsymbol{y}, z)$ and for a point source at $(\boldsymbol{x}, 0)$. In the paraxial regime it has the form

$$\hat{G}(\boldsymbol{x}, \boldsymbol{y}, z) = -\frac{ik_o}{2\pi z} \exp\Big(ik_o z + \frac{ik_o|\boldsymbol{x} - \boldsymbol{y}|^2}{2z}\Big), \tag{2}$$

where $k_o = \omega/c_o$ is the homogeneous wave number. In (1) we model the finite aperture of the detector via a Gaussian apodization function with width D, but this choice is not essential. We ask the question: how well does the imaging function $\mathcal{U}$ describe the source function f ? We will consider a detector that is large enough so that

$$r_o \ll D \text{ and } z_1 \ll k_o D^2, \tag{3}$$

where r_o is the radius of the support of the function f. The second condition means that the Rayleigh length for a beam wave with initial lateral support D is large compared to z_1, with the Rayleigh length being the range where diffraction and spreading of the beam (in the homogeneous medium) becomes significant. The transmitted field $\hat{v}$ is random due to the random section in the propagation path. If we compute the mean imaging function we find (see (61)):

$$\mathbb{E}\big[\mathcal{U}(\boldsymbol{x})\big] = \frac{1}{2\pi} \int_{\mathbb{R}^2} f\Big(\boldsymbol{x} + \frac{z_1}{k_o D}\boldsymbol{s}\Big) \exp\Big(- \frac{|\boldsymbol{s}|^2}{2}\Big) \mathrm{d}\boldsymbol{s} \exp\Big(- \frac{z_\mathrm{b} - z_\mathrm{a}}{\ell_\mathrm{sca}}\Big), \tag{4}$$

where ℓ_sca is the scattering mean free path defined in (29). Note first that the source is blurred on the classic Rayleigh resolution scale $z_1/(k_o D)$ due to the finite aperture. Thus, with infinite aperture $D = +\infty$ we recover in theory the source shape exactly, and in the homogeneous case this corresponds to time-harmonic "time reversal" and perfect refocusing at the original source location. However, the image is exponentially damped due to random scattering causing wave energy to be transferred to an incoherent wave field part. Therefore, if the thickness of the random section is large compared to the scattering mean free path ℓ_sca, then the source cannot be imaged since the coherent wave field is very small. Finally, note that the location of the random section plays no role here (only the thickness $z_\mathrm{b} - z_\mathrm{a}$ plays a role) and that imaging resolution and magnitude is not associated with any shower curtain effect. Thus, the shower curtain effect must be associated with the scattered incoherent wave part. Indeed if we consider the second-order moment or variance of the field we find that the spreading of the field depends on the location of the random section and we have a shower curtain effect in that the spreading is larger when the complex section (of fixed thickness) is farther from the source (see (31) and (41)). This spreading and the associated shower curtain effect come from random lateral scattering and affect the incoherent wave. If the random section is placed away from the source so that the wave field is subject to diffraction before it passes through the random section then this random lateral scattering effect is strong. In the optical set-up, imaging is based on the wave field intensity which

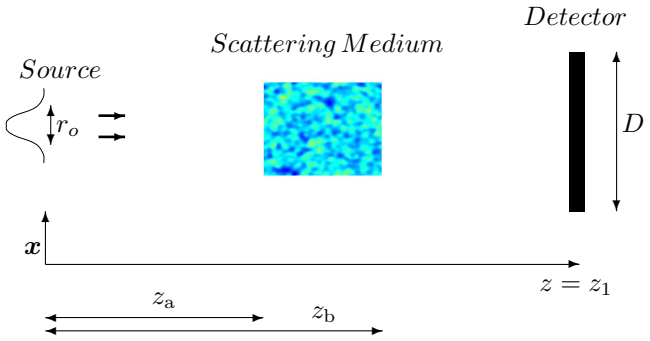

FIGURE 1. Source imaging with matched field. The detector is a receiver array that records the complex wave field.

is indeed affected by the incoherent wave component. We should therefore find a shower curtain effect for the mean image and we discuss this next.

In the optical set-up a lens is placed in the plane $z = z_1$ and the field intensity is recorded by the detector located in the plane $z = z_1 + z_2$, see Figure 2. Explicitly, the recorded intensity is

$$\mathcal{I}(\boldsymbol{x}) = \Big| \int_{\mathbb{R}^2} \hat{v}(\boldsymbol{y}, z_1)\mathcal{T}(\boldsymbol{y})\hat{G}(\boldsymbol{x}, \boldsymbol{y}, z_2)\mathrm{d}\boldsymbol{y}\Big|^2, \tag{5}$$

where $\hat{v}(\boldsymbol{y}, z_1)$ is the complex field in the plane $z = z_1$ and $\mathcal{T}(\boldsymbol{y})$ is the transmission function of the lens which is modeled by (43) corresponding to a lens aperture D and a focal length L chosen as in (45). Two situations can be distinguished. First, if the scattering is weak so that $|z_{\rm b} - z_{\rm a}| \ll \ell_{\rm sca}$, then the effect of the random section is small and the intensity recorded by the detector gives the source shape with a resolution limited only by the lens aperture. Thus, the resolution is limited by the homogeneous medium Rayleigh resolution analogous to the matched field case (see (72)). Second, if $|z_{\rm b} - z_{\rm a}| \gtrsim \ell_{\rm sca}$, then the random lateral scattering reduces the resolution. This case is interesting since the field now is incoherent and matched field imaging gives no information about the source, however, optical imaging can reveal the structure of the source. We find for the mean intensity in this strongly scattering case an expression given in (73) corresponding to a blurring on a scale being the root mean square of the Rayleigh resolution and the characteristic shower curtain resolution which is

$$R_{z_{\rm a},z_{\rm b}} = \sqrt{\frac{z_{\rm b}^3 - z_{\rm a}^3}{6\ell_{\rm par}}} = \sqrt{\frac{z_{\rm b} - z_{\rm a}}{6\ell_{\rm par}}}\sqrt{3z_{\rm a}^2 + 3z_{\rm a}(z_{\rm b} - z_{\rm a}) + (z_{\rm b} - z_{\rm a})^2}. \tag{6}$$

Here the paraxial distance $\ell_{\rm par}$ corresponds to the range of validity of the paraxial approximation (it is defined in terms of the statistics of the random medium by (38)). Thus, if the random section is close to the source then the shower curtain resolution scales like $(z_{\rm b} - z_{\rm a})\sqrt{(z_{\rm b} - z_{\rm a})/(6\ell_{\rm par})}$, while if it is far then it scales like $z_{\rm a}\sqrt{(z_{\rm b} - z_{\rm a})/(2\ell_{\rm par})}$. One may then think of the random lateral spreading as a low pass filter whose (spatial) cut off frequency becomes lower as the random section is placed farther from the source. It is important to note though that this affects the intensity pattern, but not the coherent field which is damped, but

not subject to further spreading by the random scattering. The lens can, up to the Rayleigh resolution associated with the limited aperture, compensate for the deterministic diffraction associated with the homogeneous background, however, it cannot compensate for the random wave field spreading that takes place as the wave field passes through the random section. If the random section is placed farther from the source the beam width is larger when it hits the random section and the enhanced spreading factor (of the incoherent wave field component) due to the random medium is larger. Indeed, the random medium fluctuations then happen on a scale that is narrower relative to the beam width and the lateral scattering strength is larger. In the case that the medium fluctuates only in the range z direction the shower curtain effect vanishes since broadening of the beam is then not associated with enhanced lateral scattering.

Our discussion of the optical imaging has so far been incomplete in that we have not discussed the signal-to-noise ratio of the recorded intensity pattern. Note that analyzing this involves a characterization of the variance of the intensity which is a fourth-order moment of the wave field. We push through such an analysis in the case when the source support is larger than the correlation radius of the medium fluctuations. This analysis shows that the fluctuations in the intensity pattern is as large as the mean intensity pattern in the strongly scattering regime. As specified the imaging scheme then gives only a very poor rendering of the source. We show however that by using a broadband source one can enhance the signal-to-noise ratio without sacrificing resolution. In fact the signal-to-noise ratio is characterized by

$$\mathrm{SNR} = O\left(\frac{B}{\omega_{\mathrm{c}}}\right). \tag{7}$$

Here, B is the source bandwidth and $\omega_{\mathrm{c}} = c_o \ell_{\mathrm{par}}/(z_{\mathrm{b}} - z_{\mathrm{a}})^2$ is the coherence frequency that characterizes the maximal separation distance in frequency so that the intensities recorded at two frequencies are still statistically correlated. Formula (7) shows that, if the source bandwidth is larger than this coherence frequency, then the image is statistically stable. The full quantitative description of the signal-to-noise ratio derives from (132) and (152). This result comes from the analysis of the multifrequency fourth-order moment transport equation that derives from the Itô-Schrödinger equation (16).

We remark also that in our imaging approach we have assumed that the background velocity and the range distance from the source to the detector are known. In applications related to propagation through the atmosphere it may be reasonable to assume that the background velocity is known. Estimation of the range distance to the source could be possible with detectors in several range planes or with partial knowledge of the source. We remark that the statistical structure of the transmitted field, the speckle structure, contains information also about the statistics of the random section. We do not discuss the challenge of estimating the location and structure of the random section here, but remark that a related estimation challenge is analyzed in [3] in the context of surface waves.

In the analysis presented in this paper we need to understand how scattering in the random or complex section transforms the wave field to a partly or fully incoherent wave field. In the next section we consider the white-noise paraxial approximation which describes this process for beam waves.

3. **The paraxial and Itô-Schrödinger approximations.**

We consider scalar waves and assume the governing equation:

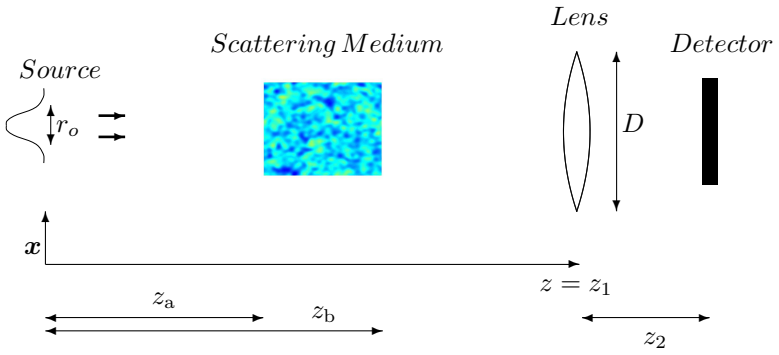

FIGURE 2. Source imaging in the optical set-up. The detector is a camera or photodetector that records the wave intensity. The source plane $z = 0$ and the detector plane $z = z_1+z_2$ are conjugate, i.e. the focal length L of the lens located in the plane $z = z_1$ satisfies (45).

$$(\partial_z^2 + \Delta_{\boldsymbol{x}})v - \frac{n^2(\boldsymbol{x}, z)}{c_o^2}\partial_t^2 v = 0, \tag{8}$$

for $(\boldsymbol{x}, z) \in \mathbb{R}^2 \times \mathbb{R}$, the space coordinates. In (8) $n(\boldsymbol{x}, z)$ is the local index of refraction. It is convenient to Fourier transform in time:

$$\hat{v}(\omega, \boldsymbol{x}, z) = \int_{\mathbb{R}} v(t, \boldsymbol{x}, z) \exp\big(i\omega t\big) \mathrm{d}t. \tag{9}$$

We then obtain the Helmholtz or reduced wave equation:

$$(\partial_z^2 + \Delta_{\boldsymbol{x}})\hat{v} + \frac{\omega^2}{c_o^2} n^2(\boldsymbol{x}, z)\hat{v} = 0, \tag{10}$$

complemented with appropriate radiation conditions. We assume a source located in the plane $z = 0$ generating a wave propagating in the positive z-direction. A particular solution of (10) in the case of a homogeneous medium $n \equiv 1$ is a propagating plane wave and we make the ansatz of a slowly-varying envelope around a plane wave going into the positive z-direction:

$$\hat{v}(\omega, \boldsymbol{x}, z) = \exp\Big(i\frac{\omega z}{c_o}\Big) u(\omega, \boldsymbol{x}, z). \tag{11}$$

In the configuration considered here, which is motivated by atmospheric propagation, there will be negligible backscattering and we can use a forward or one-way approximation, the paraxial approximation. This corresponds to assuming that u is slowly varying in z and suppressing backscattering so that u solves an initial value problem with the source at $z = 0$ being determined by the probing wave. The transverse radius of the source r_o is assumed to be *larger than the typical wavelength* while also being much *smaller than the total propagation distance*. This is the essential content of the slowly varying envelope assumption leading to the paraxial approximation. We moreover consider a scaling regime in which diffractive effects are of order one. Diffractive effects can be measured by the Rayleigh length mentioned above, defined as the distance from wave beam waist where the beam area is doubled by diffraction. In the homogeneous medium the Rayleigh length for a

beam with initial beam radius r_o and carrier wavelength λ_o is of the order of r_o^2/λ_o. Furthermore, we consider the situation when the medium is not homogeneous, but rather *fluctuating on a fine scale* and modeled in terms of a random field capturing the effect of the random section (the shower curtain). Let the local index of refraction in (8) be modeled by

$$n^2(\boldsymbol{x}, z) = 1 + \mathbf{1}_{(z_{\mathrm{a}}, z_{\mathrm{b}})}(z)\nu(\boldsymbol{x}, z), \tag{12}$$

for ν being the random medium fluctuations. We assume that ν is a stationary zero-mean random process that is mixing in z and with integrable correlations. We consider the situation in which the correlation radius of the medium is of the same order as the beam radius to capture the most delicate interaction in between the lateral fluctuations of the medium and the beam. We then get that u satisfies

$$\partial_z u = \frac{ic_o}{2\omega}\Delta_{\boldsymbol{x}} u + \frac{i\omega}{2c_o}\mathbf{1}_{(z_{\mathrm{a}}, z_{\mathrm{b}})}(z)\nu(\boldsymbol{x}, z)u, \tag{13}$$

the Schrödinger equation with a random potential, also referred to as the paraxial or forward-scattering wave equation [1, 17]. Here we assume that the potential ν has the white-noise scaling when viewed as a stochastic process in the propagation coordinate which behaves weakly (or in distribution) as a non-standard Brownian field, that is a Gaussian process with mean zero and covariance

$$\mathbb{E}[B(\boldsymbol{x}, z)B(\boldsymbol{x}', z')] = \min\{z, z'\}C(\boldsymbol{x}' - \boldsymbol{x})\,, \tag{14}$$

where the covariance $C(\boldsymbol{x})$ is given by

$$C(\boldsymbol{x}) = \int_{-\infty}^{\infty} \mathbb{E}\big[\nu(\mathbf{0}, 0)\nu(\boldsymbol{x}, z)\big]\mathrm{d}z\,. \tag{15}$$

Indeed, when the typical wavelength is much smaller than the radius of the source and correlation radius of the medium, which are themselves much smaller than the total propagation distance, then the statistical distribution of u can be approximated by that of the solution of the Itô-Schrödinger equation as analyzed in [2] and extensively used to describe physical wave propagation [16]:

$$\mathrm{d}u(\omega, \boldsymbol{x}, z) = \frac{ic_o}{2\omega}\Delta_{\boldsymbol{x}} u(\omega, \boldsymbol{x}, z)\mathrm{d}z + \frac{i\omega\mathbf{1}_{(z_{\mathrm{a}}, z_{\mathrm{b}})}(z)}{2c_o}u(\omega, \boldsymbol{x}, z) \circ \mathrm{d}B(\boldsymbol{x}, z)\,. \tag{16}$$

The symbol $\circ$ stands for the Stratonovich stochastic integral in z and $B(z, \boldsymbol{x})$ is a non-standard Brownian field or Gaussian spatial process with the covariance (14). The derivation of (16) starting from the wave equation is in [7]. In the Itô form we have

$$\begin{aligned}\mathrm{d}u(\omega, \boldsymbol{x}, z) =& \frac{ic_o}{2\omega}\Delta_{\boldsymbol{x}} u(\omega, \boldsymbol{x}, z)\mathrm{d}z - \frac{\omega^2 C(\mathbf{0})\mathbf{1}_{(z_{\mathrm{a}}, z_{\mathrm{b}})}(z)}{8c_o^2}u(\omega, \boldsymbol{x}, z)\mathrm{d}z \\ &+ \frac{i\omega\mathbf{1}_{(z_{\mathrm{a}}, z_{\mathrm{b}})}(z)}{2c_o}u(\omega, \boldsymbol{x}, z)\mathrm{d}B(\boldsymbol{x}, z)\,,\end{aligned} \tag{17}$$

where the second term on the right-hand side, corresponding to the Stratonovich corrector, captures the energy transfer from the coherent part to the incoherent part of the wave field and the exponential damping of the mean wave field. The last term in the right-hand side is the centered martingale term and does not affect the dynamics of the mean field, but it models the one of the incoherent field. The Itô-Schrödinger equation will also allow us to characterize the high-order moments.

Note that the evolution in (16) is unitary and preserves the L^2 norm corresponding to conservation of total energy as the wave propagates from the initial plane $z = 0$:

$$\int_{\mathbb{R}^2} |u(\omega, \boldsymbol{x}, z)|^2 \mathrm{d}\boldsymbol{x} = \int_{\mathbb{R}^2} |u(\omega, \boldsymbol{x}, 0)|^2 \mathrm{d}\boldsymbol{x}\,.$$

The Itô-Schrödinger equation in the context of electromagnetic waves is presented in [9]. Then the polarization modes propagate dynamically uncoupled, but they are strongly statistically coupled as the modes experience the same complex section. This means that similar estimation techniques as those presented here could be used in the case when polarization is taken into account.

4. **The mean Wigner transform.** In order to characterize the behavior of imaging algorithms based on processing of the observed wave field it is important to be able to describe moments of the wave field, that is moments when we average with respect to the driving Brownian field in (16). It turns out that in order to specifically describe the second moment of the wave it is convenient to introduce the Wigner transform. The *mean* Wigner transform is defined by

$$W_{\mathrm{m}}(\boldsymbol{r}, \boldsymbol{\xi}, z) := \int_{\mathbb{R}^2} \exp\big(-i\boldsymbol{\xi}\cdot\boldsymbol{q}\big)\mathbb{E}\Big[u\big(\boldsymbol{r}+\frac{\boldsymbol{q}}{2}, z\big)\overline{u}\big(\boldsymbol{r}-\frac{\boldsymbol{q}}{2}, z\big)\Big]\,\mathrm{d}\boldsymbol{q}. \tag{18}$$

It satisfies the closed system

$$\frac{\partial W_{\mathrm{m}}}{\partial z} + \frac{1}{k_o}\boldsymbol{\xi}\cdot\nabla_{\boldsymbol{r}} W_{\mathrm{m}} = \frac{k_o^2}{4(2\pi)^2}\mathbf{1}_{(z_{\mathrm{a}}, z_{\mathrm{b}})}(z)\int_{\mathbb{R}^2}\hat{C}(\boldsymbol{k})\Big[W_{\mathrm{m}}(\boldsymbol{\xi}-\boldsymbol{k}) - W_{\mathrm{m}}(\boldsymbol{\xi})\Big]\mathrm{d}\boldsymbol{k}, \tag{19}$$

starting from $W_{\mathrm{m}}(\boldsymbol{r}, \boldsymbol{\xi}, z = 0) = W_{\mathrm{m0}}(\boldsymbol{r}, \boldsymbol{\xi})$, which is the Wigner transform of the initial field f:

$$W_{\mathrm{m0}}(\boldsymbol{r}, \boldsymbol{\xi}) := \int_{\mathbb{R}^2} \exp\big(-i\boldsymbol{\xi}\cdot\boldsymbol{q}\big) f\big(\boldsymbol{r}+\frac{\boldsymbol{q}}{2}\big)\overline{f}\big(\boldsymbol{r}-\frac{\boldsymbol{q}}{2}\big)\mathrm{d}\boldsymbol{q}. \tag{20}$$

This result follows from the Itô-Schrödinger equation (16) using Itô calculus for Hilbert-space valued processes [22], Theorem 2.4. The transport equation (19) can be solved, first over the (homogeneous) section from 0 to z_{a}, then from z_{a} to z_{b}, and finally from z_{b} to z_1, and we find

$$\begin{aligned} W_{\mathrm{m}}(\boldsymbol{r}, \boldsymbol{\xi}, z_1) =& \frac{1}{(2\pi)^2}\iint_{\mathbb{R}^2\times\mathbb{R}^2} \exp\Big(i\boldsymbol{\zeta}\cdot\big(\boldsymbol{r} - \boldsymbol{\xi}\frac{z_1}{k_o}\big) - i\boldsymbol{\xi}\cdot\boldsymbol{q}\Big)\hat{W}_{\mathrm{m0}}(\boldsymbol{\zeta}, \boldsymbol{q}) \\ & \times \exp\Big(\frac{k_o^2}{4}\int_{z_{\mathrm{a}}}^{z_{\mathrm{b}}} C\big(\boldsymbol{q}+\boldsymbol{\zeta}\frac{z}{k_o}\big) - C(\boldsymbol{0})\mathrm{d}z\Big)\mathrm{d}\boldsymbol{\zeta}\mathrm{d}\boldsymbol{q}, \end{aligned} \tag{21}$$

where $\hat{W}_{\mathrm{m0}}$ is defined in terms of the initial field f as:

$$\hat{W}_{\mathrm{m0}}(\boldsymbol{\zeta}, \boldsymbol{q}) = \int_{\mathbb{R}^2} \exp\big(-i\boldsymbol{\zeta}\cdot\boldsymbol{r}\big) f\big(\boldsymbol{r}+\frac{\boldsymbol{q}}{2}\big)\overline{f}\big(\boldsymbol{r}-\frac{\boldsymbol{q}}{2}\big)\mathrm{d}\boldsymbol{r}. \tag{22}$$

5. **Full-aperture time-harmonic imaging.** In this section we discuss imaging when the receiver array (matched field imaging) or the lens (optical imaging) has full aperture. In the next section we discuss the case with limited aperture modeled by a Gaussian cut-off function.

5.1. **Matched field imaging.** Assume then first that we observe the complex field $u(\boldsymbol{y}, z_1)$ in the plane $z = z_1$. The matched filter imaging method consists in computing the correlation between the observed field, which is $u(\boldsymbol{y}, z_1)$, and the synthetic field generated by a point source at $\boldsymbol{x}$, which is $-\frac{ik_o}{2\pi z_1}\exp\Big(\frac{ik_o|\boldsymbol{x}-\boldsymbol{y}|^2}{2z_1}\Big)$:

$$\mathcal{U}(\boldsymbol{x}) = \frac{ik_o}{2\pi z_1}\int_{\mathbb{R}^2} u(\boldsymbol{y}, z_1)\exp\Big(-\frac{ik_o|\boldsymbol{x}-\boldsymbol{y}|^2}{2z_1}\Big)\mathrm{d}\boldsymbol{y}. \tag{23}$$

Here the synthetic field is computed in a fictitious, homogeneous medium with constant speed of propagation c_o.

Proposition 1. *If the medium is homogeneous, then the matched field image is*

$$\mathcal{U}(\boldsymbol{x}) = f(\boldsymbol{x}). \tag{24}$$

Proof. The recorded field is

$$u(\boldsymbol{x}, z_1) = -\frac{ik_o}{2\pi z_1}\int_{\mathbb{R}^2} f(\boldsymbol{y})\exp\Big(\frac{ik_o|\boldsymbol{x}-\boldsymbol{y}|^2}{2z_1}\Big)\mathrm{d}\boldsymbol{y}. \tag{25}$$

If we substitute (25) into (23), then we find

$$\begin{aligned}\mathcal{U}(\boldsymbol{x}) &= \frac{k_o^2}{(2\pi z_1)^2}\iint_{\mathbb{R}^2\times\mathbb{R}^2} f(\boldsymbol{y}')\exp\Big(i\frac{k_o|\boldsymbol{y}-\boldsymbol{y}'|^2}{2z_1} - i\frac{k_o|\boldsymbol{y}-\boldsymbol{x}|^2}{2z_1}\Big)\mathrm{d}\boldsymbol{y}'\mathrm{d}\boldsymbol{y}\\ &= \frac{k_o^2}{(2\pi z_1)^2}\iint_{\mathbb{R}^2\times\mathbb{R}^2} f(\boldsymbol{y}')\exp\Big(i\frac{k_o(|\boldsymbol{y}'|-|\boldsymbol{x}|^2)}{2z_1} + i\frac{k_o\boldsymbol{y}\cdot(\boldsymbol{x}-\boldsymbol{y}')}{z_1}\Big)\mathrm{d}\boldsymbol{y}'\mathrm{d}\boldsymbol{y}\\ &= f(\boldsymbol{x}),\end{aligned} \tag{26}$$

where we have used $\frac{k_o^2}{(2\pi z_1)^2}\int_{\mathbb{R}^2}\exp\big(i\frac{k_o\boldsymbol{y}\cdot(\boldsymbol{x}-\boldsymbol{y}')}{z_1}\big)\mathrm{d}\boldsymbol{y} = \delta(\boldsymbol{y}'-\boldsymbol{x})$. □

This proposition shows that the reconstruction of the initial field is perfect under these ideal conditions. In (23) we have assumed that the receiver array is large enough to collect the whole wave and we have

$$\int_{\mathbb{R}^2}|\mathcal{U}(\boldsymbol{x})|^2\mathrm{d}\boldsymbol{x} = \int_{\mathbb{R}^2}|u(\boldsymbol{x}, z_1)|^2\mathrm{d}\boldsymbol{x} = \int_{\mathbb{R}^2}|f(\boldsymbol{x})|^2\mathrm{d}\boldsymbol{x}. \tag{27}$$

We will address the case where the array has a limited aperture in section 6.

Let us now consider the case where the medium is randomly heterogeneous in the section $z \in (z_\mathrm{a}, z_\mathrm{b})$.

Proposition 2. *If the medium is randomly heterogeneous then the mean image is*

$$\mathbb{E}\big[\mathcal{U}(\boldsymbol{x})\big] = f(\boldsymbol{x})\exp\Big(-\frac{z_\mathrm{b}-z_\mathrm{a}}{\ell_\mathrm{sca}}\Big), \tag{28}$$

where ℓ_sca is the scattering mean free path

$$\ell_\mathrm{sca} = \frac{8}{k_o^2 C(\boldsymbol{0})}. \tag{29}$$

Proof. From (17) the mean field is the field obtained in a homogeneous medium but with an exponential damping

$$\mathbb{E}\big[u(\boldsymbol{x}, z_1)\big] = u(\boldsymbol{x}, z_1)\,|_\mathrm{homo}\exp\Big(-\frac{z_\mathrm{b}-z_\mathrm{a}}{\ell_\mathrm{sca}}\Big). \tag{30}$$

The desired results then follows. □

The expected image has the same resolution as the image obtained in homogeneous medium, one can observe only a damping. The damping depends only on the thickness $z_{\rm b}-z_{\rm a}$ of the random medium, not on its position. Matched field imaging, therefore, is not sensitive to the shower curtain effect.

The exponential damping plays an important role, because the variance of the image does not experience such damping. As we will see below, when the medium is randomly heterogeneous, the image actually looks like a speckle pattern in which the damped image of the original field is embedded.

Proposition 3. *The variance of the image* $\mathrm{Var}(\mathcal{U}(\boldsymbol{x}))=\mathbb{E}[|\mathcal{U}(\boldsymbol{x})|^2]-|\mathbb{E}[\mathcal{U}(\boldsymbol{x}))]|^2$ *is*

$$\mathrm{Var}(\mathcal{U}(\boldsymbol{x}))=\int_{\mathbb{R}^2}|f(\boldsymbol{r})|^2\mathcal{Q}(\boldsymbol{x}-\boldsymbol{r})\mathrm{d}\boldsymbol{r}, \tag{31}$$

with

$$\mathcal{Q}(\boldsymbol{r}) = \frac{1}{(2\pi)^2}\int_{\mathbb{R}^2}e^{i\boldsymbol{\zeta}\cdot\boldsymbol{r}}\Big[\exp\Big(\frac{k_o^2}{4}\int_{z_{\rm a}}^{z_{\rm b}}C(\frac{z}{k_o}\boldsymbol{\zeta})\mathrm{d}z\Big)-1\Big]\mathrm{d}\boldsymbol{\zeta}\exp\Big(-\frac{k_o^2C(\boldsymbol{0})}{4}(z_{\rm b}-z_{\rm a})\Big). \tag{32}$$

Proof. Let us consider the second-order moment

$$\begin{aligned}\mathbb{E}\big[\mathcal{U}(\boldsymbol{x})\overline{\mathcal{U}(\boldsymbol{x}')}\big] =&\frac{k_o^2}{(2\pi z_1)^2}\iint_{\mathbb{R}^2\times\mathbb{R}^2}\mathbb{E}\big[u(\boldsymbol{y},z_1)\overline{u(\boldsymbol{y}',z_1)}\big]\\ &\times\exp\Big(\frac{ik_o}{2z_1}\big(|\boldsymbol{x}'-\boldsymbol{y}'|^2-|\boldsymbol{x}-\boldsymbol{y}|^2\big)\Big)\mathrm{d}\boldsymbol{y}\mathrm{d}\boldsymbol{y}'.\end{aligned} \tag{33}$$

By (18) we can express the second moment of the wave field in terms of the mean Wigner transform:

$$\begin{aligned}&\mathbb{E}\Big[\mathcal{U}(\boldsymbol{x}+\frac{\boldsymbol{\rho}}{2})\overline{\mathcal{U}(\boldsymbol{x}-\frac{\boldsymbol{\rho}}{2})}\Big]\\ &=\frac{k_o^2}{(2\pi z_1)^2}\int_{\mathbb{R}^2}W_{\rm m}\big(\boldsymbol{r},\frac{k_o}{z_1}(\boldsymbol{r}-\boldsymbol{x}),z_1\big)\exp\Big(\frac{ik_o}{z_1}(\boldsymbol{r}-\boldsymbol{x})\cdot\boldsymbol{\rho}\Big)\mathrm{d}\boldsymbol{r}.\end{aligned} \tag{34}$$

By (21) we find

$$\begin{aligned}\mathbb{E}\Big[\mathcal{U}(\boldsymbol{x}+\frac{\boldsymbol{\rho}}{2})\overline{\mathcal{U}(\boldsymbol{x}-\frac{\boldsymbol{\rho}}{2})}\Big] =&\frac{1}{(2\pi)^2}\int_{\mathbb{R}^2}\hat{W}_{\rm m0}(\boldsymbol{\zeta},\boldsymbol{\rho})e^{i\boldsymbol{\zeta}\cdot\boldsymbol{\rho}}\\ &\times\exp\Big(\frac{k_o^2}{4}\int_{z_{\rm a}}^{z_{\rm b}}C(\boldsymbol{\rho}+\frac{z}{k_o}\boldsymbol{\zeta})-C(\boldsymbol{0})\mathrm{d}z\Big)\mathrm{d}\boldsymbol{\zeta}.\end{aligned} \tag{35}$$

The second moment of the image is

$$\begin{aligned}\mathbb{E}\big[|\mathcal{U}(\boldsymbol{x})|^2\big] &= \frac{1}{(2\pi)^2}\int_{\mathbb{R}^2}\hat{W}_{\rm m0}(\boldsymbol{\zeta},\boldsymbol{0})\exp\Big(\frac{k_o^2}{4}\int_{z_{\rm a}}^{z_{\rm b}}C(\frac{z}{k_o}\boldsymbol{\zeta})-C(\boldsymbol{0})\mathrm{d}z\Big)\mathrm{d}\boldsymbol{\zeta}\\ &=\frac{1}{(2\pi)^2}\int_{\mathbb{R}^2}|f(\boldsymbol{r})|^2\int_{\mathbb{R}^2}e^{i\boldsymbol{\zeta}\cdot(\boldsymbol{x}-\boldsymbol{r})}\exp\Big(\frac{k_o^2}{4}\int_{z_{\rm a}}^{z_{\rm b}}C(\frac{z}{k_o}\boldsymbol{\zeta})-C(\boldsymbol{0})\mathrm{d}z\Big)\mathrm{d}\boldsymbol{\zeta}\mathrm{d}\boldsymbol{r}.\end{aligned} \tag{36}$$

The variance of the image is, therefore, given by (31). □

Note in particular that

$$\int_{\mathbb{R}^2}\mathrm{Var}(\mathcal{U}(\boldsymbol{x}))\mathrm{d}\boldsymbol{x}=\int_{\mathbb{R}^2}|f(\boldsymbol{r})|^2\mathrm{d}\boldsymbol{r}\Big[1-\exp\Big(-2\frac{z_{\rm b}-z_{\rm a}}{\ell_{\rm sca}}\Big)\Big], \tag{37}$$

which expresses the conservation of energy (27): A fraction $\exp\big(-2\frac{z_\mathrm{b}-z_\mathrm{a}}{\ell_\mathrm{sca}}\big)$ of the transmitted wave energy is coherent and the rest is incoherent.

When the medium is weakly heterogeneous $z_\mathrm{b}-z_\mathrm{a} \ll \ell_\mathrm{sca}$, the image is clear $\mathbb{E}[\mathcal{U}(\boldsymbol{x})] \simeq f(\boldsymbol{x})$ and $\mathrm{Var}(\mathcal{U}(\boldsymbol{x})) \simeq 0$.

When the medium is strongly heterogeneous $z_\mathrm{b}-z_\mathrm{a} \gg \ell_\mathrm{sca}$ and C is smooth so that it can be expanded as

$$C(\boldsymbol{x}) = C(\boldsymbol{0}) - \frac{|\boldsymbol{x}|^2}{\ell_\mathrm{par}} + o(|\boldsymbol{x}|^2), \quad |\boldsymbol{x}| \to 0, \tag{38}$$

with $\ell_\mathrm{par} = -2/\Delta_{\boldsymbol{x}} C(\boldsymbol{0})$ the paraxial distance mentioned above, then the coherent component of the image is exponentially damped as shown by (28) and the noise standard deviation is significant. We have

$$\mathrm{Var}(\mathcal{U}(\boldsymbol{x})) = \int_{\mathbb{R}^2} |f(\boldsymbol{r})|^2 \mathcal{Q}(\boldsymbol{x}-\boldsymbol{r})\mathrm{d}\boldsymbol{r}, \tag{39}$$

with

$$\mathcal{Q}(\boldsymbol{r}) = \frac{3\ell_\mathrm{par}}{\pi(z_\mathrm{b}^3 - z_\mathrm{a}^3)} \exp\Big(-\frac{3\ell_\mathrm{par}|\boldsymbol{r}|^2}{(z_\mathrm{b}^3 - z_\mathrm{a}^3)}\Big). \tag{40}$$

Note that the kernel $\mathcal{Q}$ satisfies $\int_{\mathbb{R}^2} \mathcal{Q}(\boldsymbol{r})\mathrm{d}\boldsymbol{r} = 1$, so that we have $\int_{\mathbb{R}^2} \mathrm{Var}(\mathcal{U}(\boldsymbol{x}))\mathrm{d}\boldsymbol{x} = \int_{\mathbb{R}^2} |f(\boldsymbol{r})|^2 \mathrm{d}\boldsymbol{r}]$ as stated in (37). For instance, if $f(\boldsymbol{x}) = \exp(-|\boldsymbol{x}|^2/(2r_o^2))$, then

$$\mathrm{Var}(\mathcal{U}(\boldsymbol{x})) = \frac{1}{1+\frac{z_\mathrm{b}^3 - z_\mathrm{a}^3}{3r_o^2\ell_\mathrm{par}}} \exp\Big(-\frac{|\boldsymbol{x}|^2}{r_o^2\big(1+\frac{z_\mathrm{b}^3 - z_\mathrm{a}^3}{3r_o^2\ell_\mathrm{par}}\big)}\Big). \tag{41}$$

Note that the square width of the incoherent field is proportional to $z_\mathrm{b}^3 - z_\mathrm{a}^3$ which increases with z_a for a given thickness $z_\mathrm{b} - z_\mathrm{a}$. This is a first manifestation of the shower curtain effect: the spreading is larger when the complex section (of fixed thickness) is farther from the source.

5.2. **Optical imaging.** In optics it is not straightforward to observe the complex field, it is more usual to record the intensity (the square modulus of the complex field). It is then possible to propose imaging methods based on the use of a simple optical device, such as a lens, and a photodetector that records the intensity profile. This is actually the principle of the human eye and the approach we will use here.

The field is generated by a source in the plane $z = 0$, it goes through a convergent lens located in the plane $z = z_1$ and the transmitted wave is recorded in the plane $z = z_2$ by a photodetector (which records the spatially resolved intensity). The transmitted intensity in the detector plane $z = z_1 + z_2$ is

$$\mathcal{I}(\boldsymbol{x}) = \Big| -\frac{ik_o}{2\pi z_2} \int_{\mathbb{R}^2} u(\boldsymbol{y}, z_1)\mathcal{T}(\boldsymbol{y}) \exp\Big(i\frac{k_o|\boldsymbol{x}-\boldsymbol{y}|^2}{2z_2}\Big)\mathrm{d}\boldsymbol{y}\Big|^2, \tag{42}$$

where $u(\boldsymbol{y}, z_1)$ is the complex field in the plane $z = z_1$ and $\mathcal{T}(\boldsymbol{y})$ is the transmission function of the lens. A perfect, full-aperture lens has a transmission function of the form

$$\mathcal{T}(\boldsymbol{y}) = \exp\Big(-i\frac{k_o|\boldsymbol{y}|^2}{2L}\Big), \tag{43}$$

where L is the focal length of the lens.

As we will see below, when the medium is homogeneous, then we have $\mathcal{I}(\boldsymbol{x}) = |f(\boldsymbol{x})|^2$ up to magnification. When the medium is random, $\mathcal{I}(\boldsymbol{x})$ is blurred in the sense that it is a smoothed (and magnified) version of $|f(\boldsymbol{x})|^2$ and we want to quantify the blurring in this section.

In (42) we have assumed that the lens is large enough to collect the whole wave and we have

$$\int_{\mathbb{R}^2} \mathcal{I}(\boldsymbol{x})\mathrm{d}\boldsymbol{x} = \int_{\mathbb{R}^2} |u(\boldsymbol{x}, z_1)|^2 \mathrm{d}\boldsymbol{x} = \int_{\mathbb{R}^2} |f(\boldsymbol{x})|^2 \mathrm{d}\boldsymbol{x}. \tag{44}$$

We will address the case where the lens has a limited aperture in section 6.

Proposition 4. *If the photodetector is placed so that*

$$\frac{1}{L} = \frac{1}{z_1} + \frac{1}{z_2}, \tag{45}$$

and if the medium is homogeneous, then

$$\mathcal{I}(\boldsymbol{x}) = \Big| \frac{z_1}{z_2} f\Big(-\frac{z_1}{z_2}\boldsymbol{x}\Big)\Big|^2. \tag{46}$$

The condition (45) means that the detector plane $z = z_1 + z_2$ is the conjugate plane of the source plane $z = 0$ by the lens located at $z = z_1$. Proposition 4 shows that we can perfectly reconstruct the intensity profile of the initial condition. The image is inverted and magnified, and the magnification factor is $M = -z_2/z_1$. It is $M = -1$ if $z_1 = z_2$. For a typical optical device (such as the eye) we have $z_2 \ll z_1$ and the image (such as the one formed on the retina) is a reduced and inverted version of the source.

Proof. We have

$$\begin{aligned}
&\mathcal{I}(\boldsymbol{x}) \\
&= \Big| \frac{k_o^2}{(2\pi)^2 z_1 z_2} \iint_{\mathbb{R}^2\times\mathbb{R}^2} f(\boldsymbol{y}') \exp\Big(i\frac{k_o|\boldsymbol{y}-\boldsymbol{y}'|^2}{2z_1} + i\frac{k_o|\boldsymbol{y}-\boldsymbol{x}|^2}{2z_2} - i\frac{k_o|\boldsymbol{y}|^2}{2L}\Big)\mathrm{d}\boldsymbol{y}'\mathrm{d}\boldsymbol{y}\Big|^2 \\
&= \Big| \frac{k_o^2}{(2\pi)^2 z_1 z_2} \iint_{\mathbb{R}^2\times\mathbb{R}^2} f(\boldsymbol{y}') \exp\Big(i\frac{k_o|\boldsymbol{y}'|}{2z_1} + i\frac{k_o|\boldsymbol{x}|^2}{2z_2} - ik_o\boldsymbol{y}\cdot(\frac{\boldsymbol{x}}{z_2} + \frac{\boldsymbol{y}'}{z_1})\Big)\mathrm{d}\boldsymbol{y}'\mathrm{d}\boldsymbol{y}\Big|^2 \\
&= \Big| \frac{z_1}{z_2} f\Big(-\frac{z_1}{z_2}\boldsymbol{x}\Big)\Big|^2.
\end{aligned}$$

□

We next consider the mean imaging function when the medium is randomly heterogeneous and (45) holds true.

Proposition 5. *If the photodetector is placed so that (45) holds and if the medium is randomly heterogeneous, then*

$$\mathbb{E}[\mathcal{I}(\boldsymbol{x})] = \frac{z_1^2}{z_2^2}\mathcal{I}_{\mathrm{m}}\Big(-\boldsymbol{x}\frac{z_1}{z_2}\Big), \tag{47}$$

$$\mathcal{I}_{\mathrm{m}}(\boldsymbol{x}) = \int_{\mathbb{R}^2} |f(\boldsymbol{r})|^2 \mathcal{H}(\boldsymbol{x}-\boldsymbol{r})\mathrm{d}\boldsymbol{r}, \tag{48}$$

$$\mathcal{H}(\boldsymbol{x}) = \frac{1}{(2\pi)^2}\int_{\mathbb{R}^2} \exp\big(i\boldsymbol{\zeta}\cdot\boldsymbol{x}\big) \exp\Big(\frac{k_o^2}{4}\int_{z_{\mathrm{a}}}^{z_{\mathrm{b}}} C\big(\boldsymbol{\zeta}\frac{z}{k_o}\big) - C(\boldsymbol{0})\mathrm{d}z\Big)\mathrm{d}\boldsymbol{\zeta}. \tag{49}$$

This means that the image is the magnified convolution of the initial intensity distribution $|f(\boldsymbol{x})|^2$. The convolution kernel $\mathcal{H}(\boldsymbol{x})$ depends on the random medium properties. The magnification factor is $M = -z_1/z_2$.

Proof. We have

$$\mathbb{E}[\mathcal{I}(\boldsymbol{x})] = \frac{k_o^2}{(2\pi z_2)^2} \iint_{\mathbb{R}^2\times\mathbb{R}^2} \mathbb{E}\big[u(\boldsymbol{y}, z_1)\overline{u(\boldsymbol{y}', z_1)}\big] \exp\Big(-\frac{ik_o}{2L}\big(|\boldsymbol{y}|^2 - |\boldsymbol{y}'|^2\big)\Big)$$

$$\times \exp\Big(\frac{ik_o}{2z_2}\big(|\boldsymbol{x}-\boldsymbol{y}|^2-|\boldsymbol{x}-\boldsymbol{y}'|^2\big)\Big)\mathrm{d}\boldsymbol{y}\mathrm{d}\boldsymbol{y}'$$
$$= \frac{k_o^2}{(2\pi z_2)^2}\iint_{\mathbb{R}^2\times\mathbb{R}^2}\mathbb{E}\Big[u\big(\boldsymbol{r}+\frac{\boldsymbol{q}}{2},z_1\big)\overline{u}\big(\boldsymbol{r}-\frac{\boldsymbol{q}}{2},z_1\big)\Big]$$
$$\times \exp\Big(-i\frac{k_o}{L}\boldsymbol{r}\cdot\boldsymbol{q}-i\frac{k_o}{z_2}(\boldsymbol{x}-\boldsymbol{r})\cdot\boldsymbol{q}\Big)\mathrm{d}\boldsymbol{r}\mathrm{d}\boldsymbol{q},$$

which can be expressed in terms of the mean Wigner transform as

$$\mathbb{E}[\mathcal{I}(\boldsymbol{x})] = \frac{k_o^2}{(2\pi z_2)^2}\int_{\mathbb{R}^2} W_{\mathrm{m}}\big(\boldsymbol{r},\frac{k_o}{L}\boldsymbol{r}+\frac{k_o}{z_2}(\boldsymbol{x}-\boldsymbol{r}),z_1\big)\mathrm{d}\boldsymbol{r}. \tag{50}$$

By substituting the expression (21) of the mean Wigner transform we get

$$\mathbb{E}[\mathcal{I}(\boldsymbol{x})]$$
$$=\frac{k_o^2}{(2\pi)^4 z_2^2}\iiint_{\mathbb{R}^2\times\mathbb{R}^2\times\mathbb{R}^2}\hat{W}_{\mathrm{m}0}(\boldsymbol{\zeta},\boldsymbol{q})\exp\Big(i\big((1-\frac{z_1}{L})\boldsymbol{r}+\frac{z_1}{z_2}(\boldsymbol{x}-\boldsymbol{r})\big)\cdot\boldsymbol{\zeta}\Big)$$
$$\times\exp\Big(-i\big(\frac{k_o}{L}\boldsymbol{r}+\frac{k_o}{z_2}(\boldsymbol{x}-\boldsymbol{r})\big)\cdot\boldsymbol{q}+\frac{k_o^2}{4}\int_{z_{\mathrm{a}}}^{z_{\mathrm{b}}}C\big(\boldsymbol{q}+\boldsymbol{\zeta}\frac{z}{k_o}\big)-C(\boldsymbol{0})\mathrm{d}z\Big)\mathrm{d}\boldsymbol{r}\mathrm{d}\boldsymbol{\zeta}\mathrm{d}\boldsymbol{q}.$$

Using (45) and integrating in $\boldsymbol{r}$ (which generates the factor $\delta(\boldsymbol{q})$), we find

$$\mathbb{E}[\mathcal{I}(\boldsymbol{x})]$$
$$=\frac{1}{(2\pi)^2}\frac{z_1^2}{z_2^2}\int_{\mathbb{R}^2}\hat{W}_{\mathrm{m}0}(\boldsymbol{\zeta},\boldsymbol{0})\exp\Big(-i\boldsymbol{\zeta}\cdot\boldsymbol{x}\frac{z_1}{z_2}\Big)\exp\Big(\frac{k_o^2}{4}\int_{z_{\mathrm{a}}}^{z_{\mathrm{b}}}C\big(\boldsymbol{\zeta}\frac{z}{k_o}\big)-C(\boldsymbol{0})\mathrm{d}z\Big)\mathrm{d}\boldsymbol{\zeta}.$$

From the expression (22) of $\hat{W}_{\mathrm{m}0}$ we finally obtain the desired result. □

The convolution kernel (49) determines the image quality. Its radius gives the resolution of the image. In a homogeneous medium ($C\equiv 0$), it is a Dirac distribution $\delta(\boldsymbol{y})$. In a random medium,

$$\mathcal{H}(\boldsymbol{y}) = \exp\Big(-\frac{k_o^2C(\boldsymbol{0})}{4}(z_{\mathrm{b}}-z_{\mathrm{a}})\Big)\delta(\boldsymbol{y})+\frac{1}{(2\pi)^2}\int_{\mathbb{R}^2}\exp\big(i\boldsymbol{\zeta}\cdot\boldsymbol{y}\big)$$
$$\times\Big[\exp\Big(\frac{k_o^2}{4}\int_{z_{\mathrm{a}}}^{z_{\mathrm{b}}}C\big(\boldsymbol{\zeta}\frac{z}{k_o}\big)-C(\boldsymbol{0})\mathrm{d}z\Big)-\exp\Big(-\frac{k_o^2C(\boldsymbol{0})}{4}(z_{\mathrm{b}}-z_{\mathrm{a}})\Big)\Big]\mathrm{d}\boldsymbol{\zeta}. \tag{51}$$

The first term of the right-hand side is the contribution of the coherent wave and the second term is the contribution of the incoherent waves. The contribution of the coherent wave decays exponentially with the thickness $z_{\mathrm{b}}-z_{\mathrm{a}}$ of the random medium, whatever the position of the random medium in between the source plane $z=0$ and the lens plane $z=z_1$.

When $z_{\mathrm{b}}-z_{\mathrm{a}}\ll\ell_{\mathrm{sca}}$, the contribution of the coherent wave dominates and the image is good, independently on the location of the random medium.

When $z_{\mathrm{b}}-z_{\mathrm{a}}\gg\ell_{\mathrm{sca}}$, the contribution of the incoherent wave dominates. We assume now that the medium is smooth so that $C(\boldsymbol{x})$ can be expanded as (38). We then have

$$\mathcal{H}(\boldsymbol{y}) = \frac{1}{2\pi R_{z_{\mathrm{a}},z_{\mathrm{b}}}^2}\exp\Big(-\frac{|\boldsymbol{y}|^2}{2R_{z_{\mathrm{a}},z_{\mathrm{b}}}^2}\Big). \tag{52}$$

It is a Gaussian convolution kernel with radius $R_{z_{\mathrm{a}},z_{\mathrm{b}}}$ defined by (6). This result is a manifestation of the shower curtain effect (see Figure 3). For a given thickness of the random medium $z_{\mathrm{b}}-z_{\mathrm{a}}$, the radius of the convolution kernel increases with

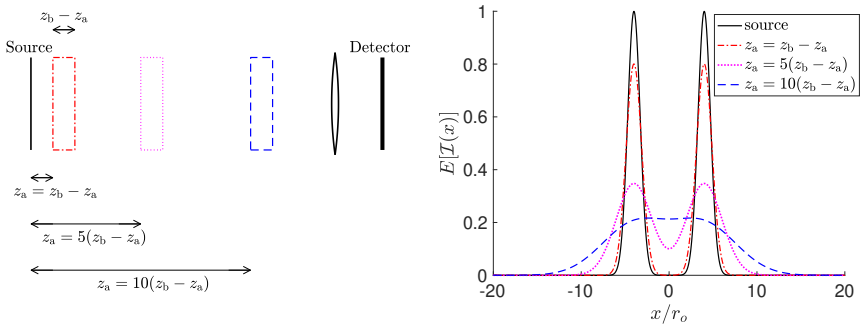

FIGURE 3. Source imaging in the optical set-up. The left picture shows the set-up with three different locations of the random section. The right picture shows the original source function and the three corresponding mean optical imaging functions. The source function is a double peak. The mean optical imaging functions are blurred versions of the source function, with a blurring that increases when the random section is farther from the source. Here we consider a two-dimensional situation, $f(x) = \exp(-(x-4r_o)^2/(2r_o^2)) + \exp(-(x+4r_o)^2/(2r_o^2))$ and $(z_b - z_a)^3/(6\ell_{\rm par}) = 0.2^2 r_o^2$.

z_a. So the image is much clearer when $z_a \simeq 0$ (the random medium is close to the source) than when $z_a \simeq z_1$ (the random medium is close to the detector).

In this section we have considered the mean imaging function. In practice we observe one realization of the imaging function $\mathcal{I}(\boldsymbol{x})$. It is therefore of interest to analyze the statistical stability of the image, which is based on the study of $\mathrm{Var}(\mathcal{I}(\boldsymbol{x}))$, which in turn involves fourth-order moments of the wave field. As we will see in Section 7, the image $\mathcal{I}(\boldsymbol{x})$ obtained in the time-harmonic regime as described in this section is not statistically stable (i.e. $\mathcal{I}(\boldsymbol{x}) \neq \mathbb{E}[\mathcal{I}(\boldsymbol{x})]$ or equivalently $\mathrm{Var}(\mathcal{I}(\boldsymbol{x})) \gtrsim \mathbb{E}[\mathcal{I}(\boldsymbol{x})]^2$). In order to get a statistically stable image (i.e. $\mathcal{I}(\boldsymbol{x}) \simeq \mathbb{E}[\mathcal{I}(\boldsymbol{x})]$ or equivalently $\mathrm{Var}(\mathcal{I}(\boldsymbol{x})) \ll \mathbb{E}[\mathcal{I}(\boldsymbol{x})]^2$) we need a self-averaging mechanism. As we will see, this can be situation when the source is broadband, and therefore the image is the superposition of many uncorrelated components, which insures the self-averaging property. This question will be addressed in section 8.

6. **Imaging with a limited aperture.** We revisit the previous section when the receiver array (matched field imaging) or the lens (optical imaging) has limited aperture. We assume that the limited aperture can be modeled by a Gaussian cut-off function with radius D.

6.1. **Matched field imaging.** The imaging function is (instead of (23)):

$$\mathcal{U}(\boldsymbol{x}) = \frac{ik_o}{2\pi z_1} \int_{\mathbb{R}^2} u(\boldsymbol{y}, z_1) \exp\Big(- \frac{ik_o|\boldsymbol{x}-\boldsymbol{y}|^2}{2z_1} - \frac{|\boldsymbol{y}|^2}{2D^2}\Big) \mathrm{d}\boldsymbol{y}. \tag{53}$$

If the medium is *homogeneous*, by substitution of (25) into (53) we obtain

$$\mathcal{U}(\boldsymbol{x}) = \frac{k_o^2 D^2}{z_1^2} \int_{\mathbb{R}^2} f(\boldsymbol{y}') \exp\Big(i\frac{k_o(|\boldsymbol{y}'| - |\boldsymbol{x}|^2)}{2z_1} - \frac{k_o^2 D^2}{2z_1^2}|\boldsymbol{x}-\boldsymbol{y}'|^2\Big) \mathrm{d}\boldsymbol{y}'$$

$$= \frac{1}{2\pi}\int_{\mathbb{R}^2} f\Big(\boldsymbol{x}+\frac{z_1}{k_oD}\boldsymbol{s}\Big)\exp\Big(-\frac{|\boldsymbol{s}|^2}{2}+i\frac{\boldsymbol{x}\cdot\boldsymbol{s}}{D}+i\frac{z_1|\boldsymbol{s}|^2}{k_oD^2}\Big)\mathrm{d}\boldsymbol{s}. \tag{54}$$

If the receiver array is large enough so that

$$r_o \ll D \text{ and } z_1 \ll k_oD^2, \tag{55}$$

where r_o is the radius of the support of f, then we get

$$\mathcal{U}(\boldsymbol{x}) = \frac{1}{2\pi}\int_{\mathbb{R}^2} f\Big(\boldsymbol{x}+\frac{z_1}{k_oD}\boldsymbol{s}\Big)\exp\Big(-\frac{|\boldsymbol{s}|^2}{2}\Big)\mathrm{d}\boldsymbol{s}. \tag{56}$$

This shows that we get a blurred image of the initial condition, with a blurring kernel that is Gaussian with radius $z_1/(k_oD)$ (the Rayleigh resolution formula). Note that, due to the fact that the array aperture is not infinite, the image energy is not equal to the energy of the initial field, but we have

$$\int_{\mathbb{R}^2}|\mathcal{U}(\boldsymbol{x})|^2\mathrm{d}\boldsymbol{x} = \frac{1}{\pi}\iint_{\mathbb{R}^2\times\mathbb{R}^2} f\big(\boldsymbol{x}+\frac{z_1}{k_oD}\boldsymbol{s}\big)\overline{f}\big(\boldsymbol{x}-\frac{z_1}{k_oD}\boldsymbol{s}\big)e^{-|\boldsymbol{s}|^2}\mathrm{d}\boldsymbol{s}\mathrm{d}\boldsymbol{x} < \int_{\mathbb{R}^2}|f(\boldsymbol{x})|^2\mathrm{d}\boldsymbol{x}, \tag{57}$$

the last inequality is due to Cauchy-Schwarz. For instance, if

$$f(\boldsymbol{x}) = \exp\Big(-\frac{|\boldsymbol{x}-\boldsymbol{x}_0|^2}{2r_o^2}\Big), \tag{58}$$

then

$$\mathcal{U}(\boldsymbol{x}) = \Big(1+\frac{z_1^2}{k_o^2D^2r_o^2}\Big)^{-1}\exp\Big(-\frac{|\boldsymbol{x}-\boldsymbol{x}_0|^2}{2r_o^2}\Big(1+\frac{z_1^2}{k_o^2D^2r_o^2}\Big)^{-1}\Big), \tag{59}$$

and

$$\int_{\mathbb{R}^2}|\mathcal{U}(\boldsymbol{x})|^2\mathrm{d}\boldsymbol{x} = \int_{\mathbb{R}^2}|f(\boldsymbol{x})|^2\mathrm{d}\boldsymbol{x}\Big(1+\frac{z_1^2}{k_o^2D^2r_o^2}\Big)^{-1}. \tag{60}$$

This shows that matched field imaging is correct as long as $z_1 < k_oDr_o$.

If the medium is *randomly heterogeneous*, then the expected image has the same expression as in the homogeneous medium, but with an additional exponential damping factor. In particular, if (55) holds true, then

$$\mathbb{E}\big[\mathcal{U}(\boldsymbol{x})\big] = \frac{1}{2\pi}\int_{\mathbb{R}^2} f\Big(\boldsymbol{x}+\frac{z_1}{k_oD}\boldsymbol{s}\Big)\exp\Big(-\frac{|\boldsymbol{s}|^2}{2}\Big)\mathrm{d}\boldsymbol{s}\exp\Big(-\frac{z_{\mathrm{b}}-z_{\mathrm{a}}}{\ell_{\mathrm{sca}}}\Big). \tag{61}$$

This shows that the coherent image energy is strongly damped:

$$\begin{aligned}\int_{\mathbb{R}^2}|\mathbb{E}[\mathcal{U}(\boldsymbol{x})]|^2\mathrm{d}\boldsymbol{x} =& \frac{1}{\pi}\iint_{\mathbb{R}^2\times\mathbb{R}^2} f\big(\boldsymbol{x}+\frac{z_1}{k_oD}\boldsymbol{s}\big)\overline{f}\big(\boldsymbol{x}-\frac{z_1}{k_oD}\boldsymbol{s}\big)e^{-|\boldsymbol{s}|^2}\mathrm{d}\boldsymbol{s}\mathrm{d}\boldsymbol{x}\\ &\times\exp\Big(-2\frac{z_{\mathrm{b}}-z_{\mathrm{a}}}{\ell_{\mathrm{sca}}}\Big).\end{aligned} \tag{62}$$

Let us consider the second moment

$$\begin{aligned}\mathbb{E}\big[|\mathcal{U}(\boldsymbol{x})|^2\big] =& \frac{k_o^2}{(2\pi z_1)^2}\iint_{\mathbb{R}^2\times\mathbb{R}^2}\mathbb{E}\big[u(\boldsymbol{y},z_1)\overline{u(\boldsymbol{y}',z_1)}\big]\\ &\times\exp\Big(\frac{ik_o}{2z_1}\big(|\boldsymbol{x}'-\boldsymbol{y}'|^2-|\boldsymbol{x}-\boldsymbol{y}|^2\big)-\frac{|\boldsymbol{y}|^2+|\boldsymbol{y}'|^2}{2D^2}\Big)\mathrm{d}\boldsymbol{y}\mathrm{d}\boldsymbol{y}'.\end{aligned} \tag{63}$$

After using (21) we find:

$$\mathbb{E}\big[|\mathcal{U}(\boldsymbol{x})|^2\big] = \frac{k_o^2D^2}{16\pi^3z_1^2}\iint_{\mathbb{R}^2\times\mathbb{R}^2}\exp\Big(i\frac{k_o}{z_1}\boldsymbol{x}\cdot\boldsymbol{q}-\frac{D^2}{4}|\frac{k_o}{z_1}\boldsymbol{q}-\boldsymbol{\zeta}|^2-\frac{|\boldsymbol{q}|^2}{4D^2}\Big)$$

$$\times \hat{W}_{\rm m0}\big(\boldsymbol{\zeta}, \boldsymbol{q} - \frac{z_1}{k_o}\boldsymbol{\zeta}\big) \exp\Big(\frac{k_o^2}{4}\int_{z_1-z_{\rm b}}^{z_1-z_{\rm a}} C(\boldsymbol{q} - \frac{z}{k_o}\boldsymbol{\zeta}) - C(\boldsymbol{0}){\rm d}z\Big){\rm d}\boldsymbol{\zeta}{\rm d}\boldsymbol{q}. \tag{64}$$

The variance of the image is, therefore,

$$\begin{aligned}
&{\rm Var}\big(\mathcal{U}(\boldsymbol{x})\big)\\
=&\frac{k_o^2 D^2}{16\pi^3 z_1^2}\iint_{\mathbb{R}^2\times\mathbb{R}^2} \exp\Big(i\frac{k_o}{z_1}\boldsymbol{x}\cdot\boldsymbol{q} - \frac{D^2}{4}\big|\frac{k_o}{z_1}\boldsymbol{q} - \boldsymbol{\zeta}\big|^2 - \frac{|\boldsymbol{q}|^2}{4D^2}\Big)\hat{W}_{\rm m0}\big(\boldsymbol{\zeta}, \boldsymbol{q} - \frac{z_1}{k_o}\boldsymbol{\zeta}\big)\\
&\times\Big[\exp\Big(\frac{k_o^2}{4}\int_{z_1-z_{\rm b}}^{z_1-z_{\rm a}} C(\boldsymbol{q} - \frac{z}{k_o}\boldsymbol{\zeta}){\rm d}z\Big) - 1\Big]{\rm d}\boldsymbol{\zeta}{\rm d}\boldsymbol{q}\exp\Big(-2\frac{z_{\rm b}-z_{\rm a}}{\ell_{\rm sca}}\Big).
\end{aligned} \tag{65}$$

As a consequence, we have

$$\begin{aligned}
\int_{\mathbb{R}^2}{\rm Var}(\mathcal{U}(\boldsymbol{x})){\rm d}\boldsymbol{x} =&\frac{D^2}{4\pi}\int_{\mathbb{R}^2}\exp\Big(-\frac{D^2}{4}|\boldsymbol{\zeta}|^2\Big)\hat{W}_{\rm m0}(\boldsymbol{\zeta}, -\frac{z_1}{k_o}\boldsymbol{\zeta})\\
&\times\Big[\exp\Big(\frac{k_o^2}{4}\int_{z_1-z_{\rm b}}^{z_1-z_{\rm a}} C(\frac{z}{k_o}\boldsymbol{\zeta}){\rm d}z\Big) - 1\Big]{\rm d}\boldsymbol{\zeta}\exp\Big(-2\frac{z_{\rm b}-z_{\rm a}}{\ell_{\rm sca}}\Big).
\end{aligned} \tag{66}$$

When the medium is weakly heterogeneous $z_{\rm b} - z_{\rm a} \ll \ell_{\rm sca}$, the image is clear ${\rm Var}(\mathcal{U}(\boldsymbol{x})) \simeq 0$.

When the medium is strongly heterogeneous $z_{\rm b} - z_{\rm a} \gg \ell_{\rm sca}$ and C is smooth so that $C(\boldsymbol{x})$ can be expanded as (38), then the mean (coherent component) of the image is exponentially damped as shown by (61) and the standard deviation is much larger than the mean as we now explain. If the initial field is (58), then we have

$$\int_{\mathbb{R}^2}{\rm Var}(\mathcal{U}(\boldsymbol{x})){\rm d}\boldsymbol{x} = \int_{\mathbb{R}^2}|f(\boldsymbol{r})|^2{\rm d}\boldsymbol{r}\Big[1 + \frac{z_1^2}{k_o^2 D^2 r_o^2} + \frac{(z_1-z_{\rm a})^3 - (z_1-z_{\rm b})^3}{3D^2\ell_{\rm par}}\Big]^{-1}. \tag{67}$$

The ratio of the coherent image energy over the incoherent image energy is

$$\frac{\int_{\mathbb{R}^2}|\mathbb{E}[\mathcal{U}(\boldsymbol{x})]|^2{\rm d}\boldsymbol{x}}{\int_{\mathbb{R}^2}{\rm Var}(\mathcal{U}(\boldsymbol{x})){\rm d}\boldsymbol{x}} = \Big[1 + \frac{(z_1-z_{\rm a})^3 - (z_1-z_{\rm b})^3}{3D^2\ell_{\rm par}\big(1 + \frac{z_1^2}{k_o^2 D^2 r_o^2}\big)}\Big]\exp\Big(-2\frac{z_{\rm b}-z_{\rm a}}{\ell_{\rm sca}}\Big), \tag{68}$$

which shows that the image quality is poor when $z_{\rm b} - z_{\rm a} \gg \ell_{\rm sca}$.

6.2. **Optical imaging.** We consider next optical imaging in the case with limited aperture. The imaging function is (42) as before, however now the transmission function of the lens is:

$$\mathcal{T}(\boldsymbol{y}) = \exp\Big(-i\frac{k_o|\boldsymbol{y}|^2}{2L} - \frac{|\boldsymbol{y}|^2}{2D^2}\Big). \tag{69}$$

The mean imaging function is given by

$$\begin{aligned}
\mathbb{E}[\mathcal{I}(\boldsymbol{x})] =&\frac{k_o^2}{(2\pi z_2)^2}\iint_{\mathbb{R}^2\times\mathbb{R}^2}\mathbb{E}\Big[u\big(\boldsymbol{r} + \frac{\boldsymbol{q}}{2}, z_1\big)\overline{u}\big(\boldsymbol{r} - \frac{\boldsymbol{q}}{2}, z_1\big)\Big]\\
&\times\exp\Big(-i\frac{k_o}{L}\boldsymbol{r}\cdot\boldsymbol{q} - i\frac{k_o}{z_2}(\boldsymbol{x}-\boldsymbol{r})\cdot\boldsymbol{q} - \frac{|\boldsymbol{r}|^2}{D^2} - \frac{|\boldsymbol{q}|^2}{4D^2}\Big){\rm d}\boldsymbol{r}{\rm d}\boldsymbol{q}.
\end{aligned} \tag{70}$$

We assume that (45) holds true and then by following the same steps as in subsection 5.2, we get that the mean imaging function has the form

$$\mathbb{E}[\mathcal{I}(\boldsymbol{x})]$$

$$=\Big(\frac{z_1}{z_2}\Big)^2\frac{k_o^2D^2}{16\pi^3z_1^2}\iint_{\mathbb{R}^2\times\mathbb{R}^2}\hat{W}_{\rm m0}(\boldsymbol{\zeta},\boldsymbol{q})\exp\Big(-\frac{k_o^2D^2|\boldsymbol{q}|^2}{4z_1^2}-\frac{|\boldsymbol{q}+\frac{z_1}{k_o}\boldsymbol{\zeta}|^2}{4D^2}\Big)$$
$$\times\exp\Big(i\big(\frac{k_o}{z_1}\boldsymbol{q}+\boldsymbol{\zeta}\big)\cdot\big(-\frac{z_1}{z_2}\boldsymbol{x}\big)+\frac{k_o^2}{4}\int_{z_{\rm a}}^{z_{\rm b}}C\big(\boldsymbol{q}+\boldsymbol{\zeta}\frac{z}{k_o}\big)-C(\boldsymbol{0})\mathrm{d}z\Big)\mathrm{d}\boldsymbol{\zeta}\mathrm{d}\boldsymbol{q}. \tag{71}$$

When $z_{\rm b}-z_{\rm a}\ll\ell_{\rm sca}$, we get the result corresponding to a homogeneous medium. If the receiver array is large enough so that (55) is satisfied, then

$$\mathbb{E}[\mathcal{I}(\boldsymbol{x})]=\mathcal{I}(\boldsymbol{x})\mid_{\rm homo}=\Big|\frac{z_1}{z_2}\frac{1}{2\pi}\int_{\mathbb{R}^2}f\Big(-\frac{z_1}{z_2}\boldsymbol{x}+\frac{z_1}{k_oD}\boldsymbol{s}\Big)\exp\Big(-\frac{|\boldsymbol{s}|^2}{2}\Big)\mathrm{d}\boldsymbol{s}\Big|^2. \tag{72}$$

This shows that the image is obtained by a blurring of the initial field with a Gaussian kernel with radius $z_1/(k_oD)$ and a magnification by the factor $M=-z_1/z_2$. The radius of the Gaussian kernel corresponds to the Rayleigh resolution formula.

When $z_{\rm b}-z_{\rm a}\gg\ell_{\rm sca}$, and the medium is smooth so that $C(\boldsymbol{x})$ can be expanded as (38), we have

$$\mathbb{E}[\mathcal{I}(\boldsymbol{x})]$$
$$=\frac{z_1^2}{z_2^2}\frac{k_o^4D^2}{4\pi^2z_1^4(a+\frac{1}{D^2})}\iint_{\mathbb{R}^2\times\mathbb{R}^2}f\big(\boldsymbol{r}+\frac{\boldsymbol{q}}{2}\big)\overline{f}\big(\boldsymbol{r}-\frac{\boldsymbol{q}}{2}\big)\exp\Big(-\frac{k_o^2|-\frac{z_1}{z_2}\boldsymbol{x}-\boldsymbol{r}|^2}{z_1^2(a+\frac{1}{D^2})}$$
$$-\frac{2ik_ob}{z_1(a+\frac{1}{D^2})}(-\frac{z_1}{z_2}\boldsymbol{x}-\boldsymbol{r})\cdot\boldsymbol{q}+i\frac{k_o}{z_1}\boldsymbol{q}\cdot\boldsymbol{r}-\big(c-\frac{b^2}{a+\frac{1}{D^2}}+\frac{k_o^2D^2}{4z_1^2}\big)|\boldsymbol{q}|^2\Big)\mathrm{d}\boldsymbol{r}\mathrm{d}\boldsymbol{q}, \tag{73}$$

with

$$a=\frac{k_o^2}{3z_1^2\ell_{\rm par}}(z_{\rm b}^3-z_{\rm a}^3), \tag{74}$$
$$b=\frac{k_o^2}{12z_1^2\ell_{\rm par}}\big[3z_1(z_{\rm b}^2-z_{\rm a}^2)-2(z_{\rm b}^3-z_{\rm a}^3)\big], \tag{75}$$
$$c=\frac{k_o^2}{12z_1^2\ell_{\rm par}}\big[3z_1^2(z_{\rm b}-z_{\rm a})-3z_1(z_{\rm b}^2-z_{\rm a}^2)+(z_{\rm b}^3-z_{\rm a}^3)\big]. \tag{76}$$

The expression (73) is complicated, but it is clear that the random medium induces blurring. For instance, if the initial condition is a sharp peak so that we can consider that $f(\boldsymbol{x})=\delta(\boldsymbol{x}-\boldsymbol{x}_0)$, then

$$\mathbb{E}[\mathcal{I}(\boldsymbol{x})]=\frac{z_1^2}{z_2^2}\frac{k_o^4D^2}{4\pi^2z_1^4(a+\frac{1}{D^2})}\exp\Big(-\frac{k_o^2|-\frac{z_1}{z_2}\boldsymbol{x}-\boldsymbol{x}_0|^2}{z_1^2(a+\frac{1}{D^2})}\Big). \tag{77}$$

Up to the magnification factor $-z_1/z_2$, this shows that the point spread function of the mean optical imaging function is a Gaussian with radius

$$\sqrt{\frac{z_1^2}{2k_o^2D^2}+\frac{az_1^2}{2k_o^2}}=\sqrt{\frac{z_1^2}{2k_o^2D^2}+\frac{z_{\rm b}^3-z_{\rm a}^3}{6\ell_{\rm par}}}, \tag{78}$$

which is the root mean square of the point spread function radius in a random medium with infinite receiver aperture and of the point spread function radius in a homogeneous medium with finite receiver aperture. This section, therefore, shows that the shower curtain effect is also noticeable with a limited receiver aperture.

7. **Statistical stability of optical imaging in the time-harmonic case.** In this section we address the question of the statistical stability of the optical imaging function. We address the full-aperture case only. We have analyzed the mean imaging function $\mathbb{E}[\mathcal{I}(\boldsymbol{x})]$ in Section 5 in the case when the field is time-harmonic. We will show in this section that the image is not statistically stable when scattering is strong. We anticipate, however, that the use of broadband source (with bandwidth smaller than the carrier frequency, but larger than a critical coherence frequency to be determined) should not affect the resolution analysis but should ensure statistical stability. In Section 8 we address the broadband case and we determine under which circumstances we can claim that $\mathcal{I}(\boldsymbol{x}) \simeq \mathbb{E}[\mathcal{I}(\boldsymbol{x})]$.

The second-order moment of the imaging function is

$$\begin{aligned}\mathbb{E}\big[\mathcal{I}(\boldsymbol{x})^2\big] =& \frac{k_o^4}{(2\pi z_2)^4}\iint_{\mathbb{R}^2\times\mathbb{R}^2\times\mathbb{R}^2\times\mathbb{R}^2} \mathrm{d}\boldsymbol{x}_1\mathrm{d}\boldsymbol{x}_2\mathrm{d}\boldsymbol{y}_1\mathrm{d}\boldsymbol{y}_2 \\ &\times \mathbb{E}\Big[u\big(\boldsymbol{x}_1,z_1\big)u\big(\boldsymbol{x}_2,z_1\big)\overline{u\big(\boldsymbol{y}_1,z_1\big)u\big(\boldsymbol{y}_2,z_1\big)}\Big] \\ &\times \exp\Big(-\frac{ik_o}{2L}\big[|\boldsymbol{x}_1|^2-|\boldsymbol{y}_1|^2+|\boldsymbol{x}_2|^2-|\boldsymbol{y}_2|^2\big]\Big) \\ &\times \exp\Big(\frac{ik_o}{2z_2}\big[|\boldsymbol{x}_1-\boldsymbol{x}|^2-|\boldsymbol{y}_1-\boldsymbol{x}|^2+|\boldsymbol{x}_2-\boldsymbol{x}|^2-|\boldsymbol{y}_2-\boldsymbol{x}|^2\big]\Big). \end{aligned} \tag{79}$$

We introduce the special Fourier transform of the fourth-order moment defined by:

$$\begin{aligned}&\hat{\mathcal{M}}_2(\boldsymbol{\xi}_1,\boldsymbol{\xi}_2,\boldsymbol{\zeta}_1,\boldsymbol{\zeta}_2,z) \\ &= \iint_{\mathbb{R}^2\times\mathbb{R}^2\times\mathbb{R}^2\times\mathbb{R}^2} \mathbb{E}\Big[u\big(\boldsymbol{x}_1,z\big)u\big(\boldsymbol{x}_2,z\big)\overline{u\big(\boldsymbol{y}_1,z\big)u\big(\boldsymbol{y}_2,z\big)}\Big] \\ &\quad\times \exp\big(-i\boldsymbol{q}_1\cdot\boldsymbol{\xi}_1-i\boldsymbol{r}_1\cdot\boldsymbol{\zeta}_1-i\boldsymbol{q}_2\cdot\boldsymbol{\xi}_2-i\boldsymbol{r}_2\cdot\boldsymbol{\zeta}_2\big)\mathrm{d}\boldsymbol{q}_1\mathrm{d}\boldsymbol{q}_2\mathrm{d}\boldsymbol{r}_1\mathrm{d}\boldsymbol{r}_2, \end{aligned} \tag{80}$$

with

$$\boldsymbol{x}_1 = \frac{\boldsymbol{r}_1+\boldsymbol{r}_2+\boldsymbol{q}_1+\boldsymbol{q}_2}{2}, \qquad \boldsymbol{y}_1 = \frac{\boldsymbol{r}_1+\boldsymbol{r}_2-\boldsymbol{q}_1-\boldsymbol{q}_2}{2}, \tag{81}$$

$$\boldsymbol{x}_2 = \frac{\boldsymbol{r}_1-\boldsymbol{r}_2+\boldsymbol{q}_1-\boldsymbol{q}_2}{2}, \qquad \boldsymbol{y}_2 = \frac{\boldsymbol{r}_1-\boldsymbol{r}_2-\boldsymbol{q}_1+\boldsymbol{q}_2}{2}. \tag{82}$$

If (45) holds true, then the second-order moment of the imaging function can be written as

$$\begin{aligned}&\mathbb{E}\big[\mathcal{I}(\boldsymbol{x})^2\big] \\ &= \frac{1}{(2\pi)^8}\Big(\frac{z_1}{z_2}\Big)^4 \iint_{\mathbb{R}^2\times\mathbb{R}^2\times\mathbb{R}^2\times\mathbb{R}^2} \mathrm{d}\boldsymbol{\xi}_1\mathrm{d}\boldsymbol{\xi}_2\mathrm{d}\boldsymbol{\zeta}_1\mathrm{d}\boldsymbol{\zeta}_2 \\ &\quad\times \hat{\mathcal{M}}_2\big(\boldsymbol{\xi}_1,\boldsymbol{\xi}_2,\boldsymbol{\zeta}_1,\boldsymbol{\zeta}_2,z_1\big)\exp\Big(2i\boldsymbol{\zeta}_1\cdot(-\frac{z_1}{z_2}\boldsymbol{x})+\frac{iz_1}{k_o}(\boldsymbol{\zeta}_1\cdot\boldsymbol{\xi}_1+\boldsymbol{\zeta}_2\cdot\boldsymbol{\xi}_2)\Big). \end{aligned} \tag{83}$$

This expression shows that it is necessary to study the fourth-order moment of the transmitted field.

7.1. **The time-harmonic fourth-order moment of the wave field.** We consider the time-harmonic fourth-order moment $M_2\big(\boldsymbol{x}_1,\boldsymbol{x}_2,\boldsymbol{y}_1,\boldsymbol{y}_2,z\big)$ defined by:

$$M_2(\boldsymbol{x}_1,\boldsymbol{x}_2,\boldsymbol{y}_1,\boldsymbol{y}_2,z) = \mathbb{E}\Big[u\big(\boldsymbol{x}_1,z\big)u\big(\boldsymbol{x}_2,z\big)\overline{u\big(\boldsymbol{y}_1,z\big)u\big(\boldsymbol{y}_2,z\big)}\Big]. \tag{84}$$

It satisfies

$$\partial_z M_2 = \frac{i}{2k_o}\Big(\Delta_{\boldsymbol{x}_1}+\Delta_{\boldsymbol{x}_2}-\Delta_{\boldsymbol{y}_1}-\Delta_{\boldsymbol{y}_2}\Big)M_2+\frac{k_o^2}{4}U_2\big(\boldsymbol{x}_1,\boldsymbol{x}_2,\boldsymbol{y}_1,\boldsymbol{y}_2\big)\mathbf{1}_{(z_\mathrm{a},z_\mathrm{b})}(z)M_2, \tag{85}$$

with the generalized potential

$$U_2(\boldsymbol{x}_1,\boldsymbol{x}_2,\boldsymbol{y}_1,\boldsymbol{y}_2) = C(\boldsymbol{x}_1-\boldsymbol{y}_1)+C(\boldsymbol{x}_1-\boldsymbol{y}_2)+C(\boldsymbol{x}_2-\boldsymbol{y}_1) + C(\boldsymbol{x}_2-\boldsymbol{y}_2)-C(\boldsymbol{x}_1-\boldsymbol{x}_2)-C(\boldsymbol{y}_1-\boldsymbol{y}_2)-2C(\boldsymbol{0}), \quad (86)$$

and it starts from $M_2(\boldsymbol{x}_1,\boldsymbol{x}_2,\boldsymbol{y}_1,\boldsymbol{y}_2,z=0) = \exp\big(-(|\boldsymbol{x}_1|^2+|\boldsymbol{y}_1|^2+|\boldsymbol{x}_2|+|\boldsymbol{y}_2|^2)/(2r_o^2)\big)$. Note that for simplicity, we here assume that the source function is of the form $f(\boldsymbol{x}) = \exp(-|\boldsymbol{x}|^2/(2r_o^2))$.

We consider the scintillation regime, that is, we assume that the radius of the initial condition (source) is much larger than the correlation radius of the random medium. We introduce a small dimensionless parameter ε in order to model this scaling regime:

$$r_o \to \frac{r_o}{\varepsilon}, \quad C \to \varepsilon C, \quad z_{\rm a} \to \frac{z_{\rm a}}{\varepsilon}, \quad z_{\rm b} \to \frac{z_{\rm b}}{\varepsilon}, \quad z_1 \to \frac{z_1}{\varepsilon}, \quad z_2 \to \frac{z_2}{\varepsilon}. \quad (87)$$

We parameterize the four points $\boldsymbol{x}_1,\boldsymbol{x}_2,\boldsymbol{y}_1,\boldsymbol{y}_2$ in (85) as in (81-82). We consider a propagation distance of the form z/ε and we denote by M_2^ε the function M_2 expressed in the variables $(\boldsymbol{q}_1,\boldsymbol{q}_2,\boldsymbol{r}_1,\boldsymbol{r}_2,z/\varepsilon)$. The function M_2^ε satisfies the equation:

$$\partial_z M_2^\varepsilon = \frac{i}{k_o\varepsilon}\big(\nabla_{\boldsymbol{r}_1}\cdot\nabla_{\boldsymbol{q}_1}+\nabla_{\boldsymbol{r}_2}\cdot\nabla_{\boldsymbol{q}_2}\big)M_2^\varepsilon + \frac{k_o^2}{4}\mathcal{U}_2(\boldsymbol{q}_1,\boldsymbol{q}_2,\boldsymbol{r}_1,\boldsymbol{r}_2)\mathbf{1}_{(z_{\rm a},z_{\rm b})}(z)M_2^\varepsilon, \quad (88)$$

with the generalized potential

$$\mathcal{U}_2(\boldsymbol{q}_1,\boldsymbol{q}_2,\boldsymbol{r}_1,\boldsymbol{r}_2) = C(\boldsymbol{q}_2+\boldsymbol{q}_1)+C(\boldsymbol{q}_2-\boldsymbol{q}_1)+C(\boldsymbol{r}_2+\boldsymbol{q}_1)+C(\boldsymbol{r}_2-\boldsymbol{q}_1) - C(\boldsymbol{q}_2+\boldsymbol{r}_2)-C(\boldsymbol{q}_2-\boldsymbol{r}_2)-2C(\boldsymbol{0}), \quad (89)$$

and where we have not written terms of order ε. The initial condition for Eq. (88) is

$$M_2^\varepsilon(\boldsymbol{q}_1,\boldsymbol{q}_2,\boldsymbol{r}_1,\boldsymbol{r}_2,z=0) = \exp\Big(-\varepsilon^2\frac{|\boldsymbol{r}_1|^2+|\boldsymbol{r}_2|^2}{2r_o^2}-\varepsilon^2\frac{|\boldsymbol{q}_1|^2+|\boldsymbol{q}_2|^2}{2r_o^2}\Big).$$

The Fourier transform (in $\boldsymbol{q}_1$, $\boldsymbol{q}_2$, $\boldsymbol{r}_1$, and $\boldsymbol{r}_2$) of the fourth-order moment is defined by:

$$\begin{aligned}&\hat{M}_2^\varepsilon\big(\boldsymbol{\xi}_1,\boldsymbol{\xi}_2,\boldsymbol{\zeta}_1,\boldsymbol{\zeta}_2,\frac{z}{\varepsilon}\big)\\ &= \iint_{\mathbb{R}^2\times\mathbb{R}^2\times\mathbb{R}^2\times\mathbb{R}^2} M_2^\varepsilon\big(\boldsymbol{q}_1,\boldsymbol{q}_2,\boldsymbol{r}_1,\boldsymbol{r}_2,\frac{z}{\varepsilon}\big)\\ &\quad\times\exp\big(-i\boldsymbol{q}_1\cdot\boldsymbol{\xi}_1-i\boldsymbol{r}_1\cdot\boldsymbol{\zeta}_1-i\boldsymbol{q}_2\cdot\boldsymbol{\xi}_2-i\boldsymbol{r}_2\cdot\boldsymbol{\zeta}_2\big)\mathrm{d}\boldsymbol{r}_1\mathrm{d}\boldsymbol{r}_2\mathrm{d}\boldsymbol{q}_1\mathrm{d}\boldsymbol{q}_2. \quad (90)\end{aligned}$$

It is clear that the first term in the right-hand side of (88) gives a rapid phase term in the equation satisfied by $\hat{M}_2^\varepsilon$. Let us absorb this rapid phase by introducing the function

$$\widetilde{M}_2^\varepsilon\big(\boldsymbol{\xi}_1,\boldsymbol{\xi}_2,\boldsymbol{\zeta}_1,\boldsymbol{\zeta}_2,\frac{z}{\varepsilon}\big) = \hat{M}_2^\varepsilon\big(\boldsymbol{\xi}_1,\boldsymbol{\xi}_2,\boldsymbol{\zeta}_1,\boldsymbol{\zeta}_2,\frac{z}{\varepsilon}\big)\exp\Big(\frac{iz}{k_o\varepsilon}(\boldsymbol{\xi}_2\cdot\boldsymbol{\zeta}_2+\boldsymbol{\xi}_1\cdot\boldsymbol{\zeta}_1)\Big). \quad (91)$$

In the scintillation regime the rescaled function $\widetilde{M}_2^\varepsilon$ satisfies the equation with fast phases

$$\begin{aligned}\partial_z\widetilde{M}_2^\varepsilon = &\frac{k_o^2}{4(2\pi)^2}\mathbf{1}_{(z_{\rm a},z_{\rm b})}(z)\int_{\mathbb{R}^2}\hat{C}(\boldsymbol{k})\Big[-2\widetilde{M}_2^\varepsilon(\boldsymbol{\xi}_1,\boldsymbol{\xi}_2,\boldsymbol{\zeta}_1,\boldsymbol{\zeta}_2)\\ &+\widetilde{M}_2^\varepsilon(\boldsymbol{\xi}_1-\boldsymbol{k},\boldsymbol{\xi}_2-\boldsymbol{k},\boldsymbol{\zeta}_1,\boldsymbol{\zeta}_2)e^{i\frac{z}{\varepsilon k_o}\boldsymbol{k}\cdot(\boldsymbol{\zeta}_2+\boldsymbol{\zeta}_1)}\\ &+\widetilde{M}_2^\varepsilon(\boldsymbol{\xi}_1-\boldsymbol{k},\boldsymbol{\xi}_2,\boldsymbol{\zeta}_1,\boldsymbol{\zeta}_2-\boldsymbol{k})e^{i\frac{z}{\varepsilon k_o}\boldsymbol{k}\cdot(\boldsymbol{\xi}_2+\boldsymbol{\zeta}_1)}\\ &+\widetilde{M}_2^\varepsilon(\boldsymbol{\xi}_1+\boldsymbol{k},\boldsymbol{\xi}_2-\boldsymbol{k},\boldsymbol{\zeta}_1,\boldsymbol{\zeta}_2)e^{i\frac{z}{\varepsilon k_o}\boldsymbol{k}\cdot(\boldsymbol{\zeta}_2-\boldsymbol{\zeta}_1)}\end{aligned}$$

$$+\widetilde{M}_2^\varepsilon(\boldsymbol{\xi}_1+\boldsymbol{k},\boldsymbol{\xi}_2,\boldsymbol{\zeta}_1,\boldsymbol{\zeta}_2-\boldsymbol{k})e^{i\frac{z}{\varepsilon k_o}\boldsymbol{k}\cdot(\boldsymbol{\xi}_2-\boldsymbol{\zeta}_1)}$$
$$-\widetilde{M}_2^\varepsilon(\boldsymbol{\xi}_1,\boldsymbol{\xi}_2-\boldsymbol{k},\boldsymbol{\zeta}_1,\boldsymbol{\zeta}_2-\boldsymbol{k})e^{i\frac{z}{\varepsilon k_o}(\boldsymbol{k}\cdot(\boldsymbol{\zeta}_2+\boldsymbol{\xi}_2)-|\boldsymbol{k}|^2)}$$
$$-\widetilde{M}_2^\varepsilon(\boldsymbol{\xi}_1,\boldsymbol{\xi}_2-\boldsymbol{k},\boldsymbol{\zeta}_1,\boldsymbol{\zeta}_2+\boldsymbol{k})e^{i\frac{z}{\varepsilon k_o}(\boldsymbol{k}\cdot(\boldsymbol{\zeta}_2-\boldsymbol{\xi}_2)+|\boldsymbol{k}|^2)}\Big]\mathrm{d}\boldsymbol{k}, \tag{92}$$

starting from $\widetilde{M}_2^\varepsilon(\boldsymbol{\xi}_1,\boldsymbol{\xi}_2,\boldsymbol{\zeta}_1,\boldsymbol{\zeta}_2,z=0)=(2\pi)^8\phi_{r_o}^\varepsilon(\boldsymbol{\xi}_1)\phi_{r_o}^\varepsilon(\boldsymbol{\xi}_2)\phi_{r_o}^\varepsilon(\boldsymbol{\zeta}_1)\phi_{r_o}^\varepsilon(\boldsymbol{\zeta}_2)$, where $\phi_{r_o}^\varepsilon$ is defined by

$$\phi_{r_o}^\varepsilon(\boldsymbol{\xi})=\frac{r_o^2}{2\pi\varepsilon^2}\exp\Big(-\frac{r_o^2|\boldsymbol{\xi}|^2}{2\varepsilon^2}\Big). \tag{93}$$

The following result shows that $\widetilde{M}_2^\varepsilon$ exhibits a multi-scale behavior as $\varepsilon\to 0$, with some components evolving at the scale ε and some components evolving at the scale 1.

Proposition 6. *The function $\widetilde{M}_2^\varepsilon(\boldsymbol{\xi}_1,\boldsymbol{\xi}_2,\boldsymbol{\zeta}_1,\boldsymbol{\zeta}_2,z/\varepsilon)$ can be expanded as*

$$\begin{aligned}
&\widetilde{M}_2^\varepsilon\big(\boldsymbol{\xi}_1,\boldsymbol{\xi}_2,\boldsymbol{\zeta}_1,\boldsymbol{\zeta}_2,\frac{z}{\varepsilon}\big)\\
=\;& K(z)^2\phi_{r_o}^\varepsilon(\boldsymbol{\xi}_1)\phi_{r_o}^\varepsilon(\boldsymbol{\xi}_2)\phi_{r_o}^\varepsilon(\boldsymbol{\zeta}_1)\phi_{r_o}^\varepsilon(\boldsymbol{\zeta}_2)\\
&+\frac{K(z)}{2}\phi_{r_o}^\varepsilon\big(\frac{\boldsymbol{\xi}_1-\boldsymbol{\xi}_2}{\sqrt{2}}\big)\phi_{r_o}^\varepsilon(\boldsymbol{\zeta}_1)\phi_{r_o}^\varepsilon(\boldsymbol{\zeta}_2)A\big(z,\frac{\boldsymbol{\xi}_2+\boldsymbol{\xi}_1}{2},\frac{\boldsymbol{\zeta}_2+\boldsymbol{\zeta}_1}{\varepsilon}\big)\\
&+\frac{K(z)}{2}\phi_{r_o}^\varepsilon\big(\frac{\boldsymbol{\xi}_1+\boldsymbol{\xi}_2}{\sqrt{2}}\big)\phi_{r_o}^\varepsilon(\boldsymbol{\zeta}_1)\phi_{r_o}^\varepsilon(\boldsymbol{\zeta}_2)A\big(z,\frac{\boldsymbol{\xi}_2-\boldsymbol{\xi}_1}{2},\frac{\boldsymbol{\zeta}_2-\boldsymbol{\zeta}_1}{\varepsilon}\big)\\
&+\frac{K(z)}{2}\phi_{r_o}^\varepsilon\big(\frac{\boldsymbol{\xi}_1-\boldsymbol{\zeta}_2}{\sqrt{2}}\big)\phi_{r_o}^\varepsilon(\boldsymbol{\zeta}_1)\phi_{r_o}^\varepsilon(\boldsymbol{\xi}_2)A\big(z,\frac{\boldsymbol{\zeta}_2+\boldsymbol{\xi}_1}{2},\frac{\boldsymbol{\xi}_2+\boldsymbol{\zeta}_1}{\varepsilon}\big)\\
&+\frac{K(z)}{2}\phi_{r_o}^\varepsilon\big(\frac{\boldsymbol{\xi}_1+\boldsymbol{\zeta}_2}{\sqrt{2}}\big)\phi_{r_o}^\varepsilon(\boldsymbol{\zeta}_1)\phi_{r_o}^\varepsilon(\boldsymbol{\xi}_2)A\big(z,\frac{\boldsymbol{\zeta}_2-\boldsymbol{\xi}_1}{2},\frac{\boldsymbol{\xi}_2-\boldsymbol{\zeta}_1}{\varepsilon}\big)\\
&+\frac{1}{4}\phi_{r_o}^\varepsilon(\boldsymbol{\zeta}_1)\phi_{r_o}^\varepsilon(\boldsymbol{\zeta}_2)A\big(z,\frac{\boldsymbol{\xi}_2+\boldsymbol{\xi}_1}{2},\frac{\boldsymbol{\zeta}_2+\boldsymbol{\zeta}_1}{\varepsilon}\big)A\big(z,\frac{\boldsymbol{\xi}_2-\boldsymbol{\xi}_1}{2},\frac{\boldsymbol{\zeta}_2-\boldsymbol{\zeta}_1}{\varepsilon}\big)\\
&+\frac{1}{4}\phi_{r_o}^\varepsilon(\boldsymbol{\zeta}_1)\phi_{r_o}^\varepsilon(\boldsymbol{\xi}_2)A\big(z,\frac{\boldsymbol{\zeta}_2+\boldsymbol{\xi}_1}{2},\frac{\boldsymbol{\xi}_2+\boldsymbol{\zeta}_1}{\varepsilon}\big)A\big(z,\frac{\boldsymbol{\zeta}_2-\boldsymbol{\xi}_1}{2},\frac{\boldsymbol{\xi}_2-\boldsymbol{\zeta}_1}{\varepsilon}\big)\\
&+R_2^\varepsilon(z,\boldsymbol{\xi}_1,\boldsymbol{\xi}_2,\boldsymbol{\zeta}_1,\boldsymbol{\zeta}_2),
\end{aligned} \tag{94}$$

where the function K is defined by

$$K(z)=(2\pi)^4\exp\Big(-\frac{k_o^2}{4}C(\boldsymbol{0})\min((z_{\rm b}-z_{\rm a}),(z-z_{\rm a})_+)\Big), \tag{95}$$

the function $(z,\boldsymbol{\xi})\mapsto A(z,\boldsymbol{\xi},\boldsymbol{\zeta})$ is the solution of

$$\begin{aligned}
\partial_z A \;=\;& \frac{k_o^2}{4(2\pi)^2}\mathbf{1}_{(z_{\rm a},z_{\rm b})}(z)\int_{\mathbb{R}^2}\hat{C}(\boldsymbol{k})\big[A(\boldsymbol{\xi}-\boldsymbol{k})e^{\frac{iz}{k_o}\boldsymbol{k}\cdot\boldsymbol{\zeta}}-A(\boldsymbol{\xi})\big]\mathrm{d}\boldsymbol{k}\\
&+\frac{k_o^2}{4(2\pi)^2}K(z)\mathbf{1}_{(z_{\rm a},z_{\rm b})}(z)\hat{C}(\boldsymbol{\xi})e^{\frac{iz}{k_o}\boldsymbol{\xi}\cdot\boldsymbol{\zeta}},
\end{aligned} \tag{96}$$

starting from $A(z=0,\boldsymbol{\xi},\boldsymbol{\zeta})=0$, and the function R_2^ε satisfies

$$\sup_{z\in[0,z_1]}\|R_2^\varepsilon(z,\cdot,\cdot,\cdot,\cdot)\|_{L^1(\mathbb{R}^2\times\mathbb{R}^2\times\mathbb{R}^2\times\mathbb{R}^2)}\overset{\varepsilon\to 0}{\longrightarrow}0. \tag{97}$$

This result was already formulated in Proposition 6.1 in [8]. It shows that, if we deal with an integral of $\widetilde{M}_2^\varepsilon$ against a bounded function, then we can replace $\widetilde{M}_2^\varepsilon$

by the right-hand side of (94) without the R_2^ε term up to a negligible error when ε is small.

7.2. **The second-order moment of the optical imaging function in the time-harmonic case.** We again consider the scintillation regime, that is, we assume that the radius of the initial condition is much larger than the correlation radius of the random medium. We introduce a small dimensionless parameter ε in order to model this scaling regime as in (87).

Proposition 7. *When $\varepsilon \to 0$, the mean optical imaging function is*

$$\begin{aligned}&\mathbb{E}\big[\mathcal{I}(\frac{\boldsymbol{x}}{\varepsilon})\big]\\ &=\Big(\frac{z_1}{z_2}\Big)^2\frac{r_o^2}{4\pi}\int_{\mathbb{R}^2}\mathrm{d}\boldsymbol{\zeta}\exp\Big(i\boldsymbol{\zeta}\cdot(-\frac{z_1}{z_2}\boldsymbol{x})-\frac{r_o^2|\boldsymbol{\zeta}|^2}{4}+\frac{k_o^2}{4}\int_{z_{\mathrm{a}}}^{z_{\mathrm{b}}}C\big(\boldsymbol{\zeta}\frac{z}{k_o}\big)-C(\mathbf{0})\mathrm{d}z\Big)\end{aligned}\tag{98}$$

and its variance is

$$\begin{aligned}&\mathrm{Var}\big(\mathcal{I}(\frac{\boldsymbol{x}}{\varepsilon})\big)\\ &=\Big(\frac{z_1}{z_2}\Big)^4\Big|\int_{\mathbb{R}^2}\mathrm{d}\boldsymbol{\alpha}\exp\big(i\boldsymbol{\alpha}\cdot(-\frac{z_1}{z_2}\boldsymbol{x})\big)\phi^1_{\frac{r_o}{\sqrt{2}}}(\boldsymbol{\alpha})\exp\Big(\frac{k_o^2}{4}\int_{z_{\mathrm{a}}}^{z_{\mathrm{b}}}C(\boldsymbol{\alpha}\frac{z}{k_o})-C(\mathbf{0})\mathrm{d}z\Big)\Big|^2\\ &\quad-\Big(\frac{z_1}{z_2}\Big)^4\Big|\int_{\mathbb{R}^2}\mathrm{d}\boldsymbol{\alpha}\exp\big(i\boldsymbol{\alpha}\cdot(-\frac{z_1}{z_2}\boldsymbol{x})\big)\phi^1_{\frac{r_o}{\sqrt{2}}}(\boldsymbol{\alpha})\exp\Big(-\frac{k_o^2}{4}C(\mathbf{0})(z_{\mathrm{b}}-z_{\mathrm{a}})\Big)\Big|^2.\end{aligned}\tag{99}$$

Proof. First, the expression of the mean follows from (71) in the scaling regime (87). Second, we find that the second-order moment of the optical imaging function is

$$\begin{aligned}&\mathbb{E}\big[\mathcal{I}(\frac{\boldsymbol{x}}{\varepsilon})^2\big]\\ &=\frac{1}{(2\pi)^8}\Big(\frac{z_1}{z_2}\Big)^4\int_{\mathbb{R}^2}\mathrm{d}\boldsymbol{\zeta}_1\exp\big(2i\boldsymbol{\zeta}_1\cdot(-\frac{z_1}{z_2}\boldsymbol{x})\big)\phi^1_{r_o}(\boldsymbol{\zeta}_1)\Big\{K(z_1)^2\\ &\quad+K(z_1)\iint_{\mathbb{R}^2\times\mathbb{R}^2}\mathrm{d}\boldsymbol{\zeta}_2\mathrm{d}\boldsymbol{\xi}_2\phi^1_{r_o}(\boldsymbol{\zeta}_2)\big[A\big(z_1,\boldsymbol{\xi}_2,\boldsymbol{\zeta}_2+\boldsymbol{\zeta}_1\big)+A\big(z_1,\boldsymbol{\xi}_2,\boldsymbol{\zeta}_2-\boldsymbol{\zeta}_1\big)\big]\\ &\quad+K(z_1)\iint_{\mathbb{R}^2\times\mathbb{R}^2}\mathrm{d}\boldsymbol{\zeta}_2\mathrm{d}\boldsymbol{\xi}_2\phi^1_{r_o}(\boldsymbol{\xi}_2)A\big(z_1,\boldsymbol{\zeta}_2,\boldsymbol{\xi}_2+\boldsymbol{\zeta}_1\big)\\ &\quad+K(z_1)\iint_{\mathbb{R}^2\times\mathbb{R}^2}\mathrm{d}\boldsymbol{\zeta}_2\mathrm{d}\boldsymbol{\xi}_2\phi^1_{r_o}(\boldsymbol{\xi}_2)A\big(z_1,\boldsymbol{\zeta}_2,\boldsymbol{\xi}_2-\boldsymbol{\zeta}_1\big)\\ &\quad+\frac{1}{4}\iint_{\mathbb{R}^2\times\mathbb{R}^2\times\mathbb{R}^2}\mathrm{d}\boldsymbol{\zeta}_2\mathrm{d}\boldsymbol{\xi}_1\mathrm{d}\boldsymbol{\xi}_2\phi^1_{r_o}(\boldsymbol{\zeta}_2)A\big(z_1,\frac{\boldsymbol{\xi}_2+\boldsymbol{\xi}_1}{2},\boldsymbol{\zeta}_2+\boldsymbol{\zeta}_1\big)A\big(z_1,\frac{\boldsymbol{\xi}_2-\boldsymbol{\xi}_1}{2},\boldsymbol{\zeta}_2-\boldsymbol{\zeta}_1\big)\\ &\quad+\frac{1}{4}\iint_{\mathbb{R}^2\times\mathbb{R}^2\times\mathbb{R}^2}\mathrm{d}\boldsymbol{\zeta}_2\mathrm{d}\boldsymbol{\xi}_1\mathrm{d}\boldsymbol{\xi}_2\phi^1_{r_o}(\boldsymbol{\xi}_2)A\big(z_1,\frac{\boldsymbol{\zeta}_2+\boldsymbol{\xi}_1}{2},\boldsymbol{\xi}_2+\boldsymbol{\zeta}_1\big)A\big(z_1,\frac{\boldsymbol{\zeta}_2-\boldsymbol{\xi}_1}{2},\boldsymbol{\xi}_2-\boldsymbol{\zeta}_1\big)\Big\}.\end{aligned}$$

Therefore we can write

$$\begin{aligned}&\mathrm{Var}\big(\mathcal{I}(\frac{\boldsymbol{x}}{\varepsilon})\big)\\ &=\frac{1}{(2\pi)^8}\Big(\frac{z_1}{z_2}\Big)^4\int_{\mathbb{R}^2}\mathrm{d}\boldsymbol{\zeta}_1\exp\big(2i\boldsymbol{\zeta}_1\cdot(-\frac{z_1}{z_2}\boldsymbol{x})\big)\phi^1_{r_o}(\boldsymbol{\zeta}_1)\\ &\quad\times\Big\{K(z_1)\iint_{\mathbb{R}^2\times\mathbb{R}^2}\mathrm{d}\boldsymbol{\zeta}_2\mathrm{d}\boldsymbol{\xi}_2\phi^1_{r_o}(\boldsymbol{\zeta}_2)\big[A\big(z_1,\boldsymbol{\xi}_2,\boldsymbol{\zeta}_2+\boldsymbol{\zeta}_1\big)+A\big(z_1,\boldsymbol{\xi}_2,\boldsymbol{\zeta}_2-\boldsymbol{\zeta}_1\big)\big]\\ &\quad+\frac{1}{4}\iint_{\mathbb{R}^2\times\mathbb{R}^2\times\mathbb{R}^2}\mathrm{d}\boldsymbol{\zeta}_2\mathrm{d}\boldsymbol{\xi}_1\mathrm{d}\boldsymbol{\xi}_2\phi^1_{r_o}(\boldsymbol{\zeta}_2)A\big(z_1,\frac{\boldsymbol{\xi}_2+\boldsymbol{\xi}_1}{2},\boldsymbol{\zeta}_2+\boldsymbol{\zeta}_1\big)\\ &\qquad A\big(z_1,\frac{\boldsymbol{\xi}_2-\boldsymbol{\xi}_1}{2},\boldsymbol{\zeta}_2-\boldsymbol{\zeta}_1\big)\Big\},\end{aligned}$$

or

$$\mathrm{Var}\big(\mathcal{I}(\frac{\boldsymbol{x}}{\varepsilon})\big) = \frac{1}{(2\pi)^8}\Big(\frac{z_1}{z_2}\Big)^4 \iint_{\mathbb{R}^2\times\mathbb{R}^2} \mathrm{d}\boldsymbol{\alpha}\mathrm{d}\boldsymbol{\beta} \exp\big(i(\boldsymbol{\alpha}-\boldsymbol{\beta})\cdot(-\frac{z_1}{z_2}\boldsymbol{x})\big)\phi^1_{\frac{r_o}{\sqrt{2}}}(\boldsymbol{\alpha})\phi^1_{\frac{r_o}{\sqrt{2}}}(\boldsymbol{\beta}) \\ \times\Big\{K(z_1)E\big(z_1,\boldsymbol{\alpha}\big)+K(z_1)E\big(z_1,\boldsymbol{\beta}\big)+E\big(z_1,\boldsymbol{\alpha}\big)E\big(z_1,\boldsymbol{\beta}\big)\Big\}, \tag{100}$$

with

$$E(z,\boldsymbol{\zeta}) = \int_{\mathbb{R}^2} A(z,\boldsymbol{\xi},\boldsymbol{\zeta})\mathrm{d}\boldsymbol{\xi}. \tag{101}$$

From (96) the function E satisfies the ordinary differential equation (in which $\boldsymbol{\zeta}$ is frozen)

$$\partial_z E = \frac{k_o^2}{4}\mathbf{1}_{(z_{\mathrm{a}},z_{\mathrm{b}})}(z)\Big[C\big(\boldsymbol{\zeta}\frac{z}{k_o}\big)-1\Big]E + \frac{k_o^2}{4}K(z)\mathbf{1}_{(z_{\mathrm{a}},z_{\mathrm{b}})}(z)C\big(\boldsymbol{\zeta}\frac{z}{k_o}\big), \tag{102}$$

starting from $E(z=0,\boldsymbol{\zeta})=0$, which makes it possible to obtain a closed-form expression:

$$E(z_1,\boldsymbol{\zeta}) = (2\pi)^4\Big[\exp\Big(\frac{k_o^2}{4}\int_{z_{\mathrm{a}}}^{z_{\mathrm{b}}} C(\boldsymbol{\zeta}\frac{z}{k_o})\mathrm{d}z\Big)-1\Big]\exp\Big(-\frac{k_o^2 C(\mathbf{0})(z_{\mathrm{b}}-z_{\mathrm{a}})}{4}\Big). \tag{103}$$

Substituting this into (100) we obtain the expression of the variance of the optical imaging function (99). □

In the strongly scattering regime the expressions of the mean and variance of the optical imaging function become simpler and we study this situation in the next subsection.

7.3. **The second-order moment of the optical imaging function in the time-harmonic case and in the strongly scattering regime.** In the strongly scattering regime, when $z_{\mathrm{b}}-z_{\mathrm{a}} \gg \ell_{\mathrm{sca}}$ and the random medium is smooth so that $C(\boldsymbol{x})$ can be expanded as (38), then the mean optical imaging function is

$$\mathbb{E}\big[\mathcal{I}(\frac{\boldsymbol{x}}{\varepsilon})\big] = \Big(\frac{z_1}{z_2}\Big)^2 \frac{1}{1+\frac{z_{\mathrm{b}}^3-z_{\mathrm{a}}^3}{3r_o^2\ell_{\mathrm{par}}}} \exp\Big(-\frac{|-\frac{z_1}{z_2}\boldsymbol{x}|^2}{r_o^2+\frac{z_{\mathrm{b}}^3-z_{\mathrm{a}}^3}{3\ell_{\mathrm{par}}}}\Big), \tag{104}$$

and its variance is of the form

$$\mathrm{Var}\big(\mathcal{I}(\frac{\boldsymbol{x}}{\varepsilon})\big) = \Big(\frac{z_1}{z_2}\Big)^4 \frac{1}{\big(1+\frac{z_{\mathrm{b}}^3-z_{\mathrm{a}}^3}{3r_o^2\ell_{\mathrm{par}}}\big)^2} \exp\Big(-\frac{2|-\frac{z_1}{z_2}\boldsymbol{x}|^2}{r_o^2+\frac{z_{\mathrm{b}}^3-z_{\mathrm{a}}^3}{3\ell_{\mathrm{par}}}}\Big),$$

that is to say,

$$\mathrm{Var}\big(\mathcal{I}(\frac{\boldsymbol{x}}{\varepsilon})\big) = \mathbb{E}\big[\mathcal{I}(\frac{\boldsymbol{x}}{\varepsilon})\big]^2. \tag{105}$$

This shows that the fluctuations are of the same order of magnitude as the mean image, in other words, the image is not stable.

8. **Stability in the broadband regime.** We consider here an initial condition of the form

$$f(\boldsymbol{x},t) = \exp\Big(-\frac{|\boldsymbol{x}|^2}{2r_o^2}\Big)g(t) + c.c., \tag{106}$$

where $g(t)$ is a time profile with central frequency ω_o and bandwidth B, so that its Fourier transform has the form:

$$\hat{g}(\omega) = \frac{1}{\sqrt{B}}\hat{g}_0\Big(\frac{\omega-\omega_o}{B}\Big). \tag{107}$$

The time-dependent transmitted field at $z = z_1$ is

$$\frac{1}{2\pi}\int_{\mathbb{R}} u(\omega, \boldsymbol{x}, z_1)e^{-i\omega t}\mathrm{d}\omega + c.c., \tag{108}$$

where $u(\omega, \boldsymbol{x}, z)$ is solution of the Itô-Schrödinger equation (in which ω is frozen) starting from

$$u(\omega, \boldsymbol{x}, z = 0) = \exp\Big(-\frac{|\boldsymbol{x}|^2}{2r_o^2}\Big)\hat{g}(\omega). \tag{109}$$

The optical imaging function is the spatially resolved wave energy recorded by the photodetector in the plane $z = z_2$:

$$\mathcal{I}(\boldsymbol{x}) = \int_{\mathbb{R}} \mathrm{d}t\Big|\int_{\mathbb{R}} \mathrm{d}\omega \frac{ik(\omega)}{2\pi z_2}\int_{\mathbb{R}^2} \mathrm{d}\boldsymbol{y} u(\omega, \boldsymbol{y}, z_1)\exp\Big(i\frac{k(\omega)|\boldsymbol{x}-\boldsymbol{y}|^2}{2z_2} - i\frac{k(\omega)|\boldsymbol{y}|^2}{2L} - i\omega t\Big)\Big|^2, \tag{110}$$

where $k(\omega) = \omega/c_o$. By Parseval's formula this can also be written as:

$$\mathcal{I}(\boldsymbol{x}) = \int_{\mathbb{R}} \frac{\mathrm{d}\omega}{2\pi}\Big|\frac{k(\omega)}{2\pi z_2}\int_{\mathbb{R}^2} \mathrm{d}\boldsymbol{y} u(\omega, \boldsymbol{y}, z_1)\exp\Big(i\frac{k(\omega)|\boldsymbol{x}-\boldsymbol{y}|^2}{2z_2} - i\frac{k(\omega)|\boldsymbol{y}|^2}{2L}\Big)\Big|^2. \tag{111}$$

As a consequence, if (45) holds true, then the mean imaging function is

$$\mathbb{E}\big[\mathcal{I}(\boldsymbol{x})\big] = \Big(\frac{z_1}{z_2}\Big)^2 \mathcal{I}_{\mathrm{m}}\Big(-\frac{z_1}{z_2}\boldsymbol{x}\Big), \tag{112}$$

$$\mathcal{I}_{\mathrm{m}}(\boldsymbol{x}) = \int_{\mathbb{R}^2}\Big|\exp\Big(-\frac{|\boldsymbol{r}|^2}{2r_o^2}\Big)\Big|^2 \mathcal{H}(\boldsymbol{x}-\boldsymbol{r})\mathrm{d}\boldsymbol{r}, \tag{113}$$

with the convolution kernel

$$\mathcal{H}(\boldsymbol{x}) = \int_{\mathbb{R}} \frac{\mathrm{d}\omega}{2\pi}\frac{|\hat{g}(\omega)|^2}{(2\pi)^2}\int_{\mathbb{R}^2} \mathrm{d}\boldsymbol{\zeta}\exp\big(i\boldsymbol{\zeta}\cdot\boldsymbol{x}\big)\exp\Big(\frac{k(\omega)^2}{4}\int_{z_{\mathrm{a}}}^{z_{\mathrm{b}}} C\big(\boldsymbol{\zeta}\frac{z}{k(\omega)}\big) - C(\boldsymbol{0})\mathrm{d}z\Big). \tag{114}$$

If $\hat{g}$ is of the form (107) and the bandwidth B is smaller than the central frequency ω_o, then we have simply

$$\mathcal{H}(\boldsymbol{x}) = \Big[\int_{\mathbb{R}} \frac{\mathrm{d}\omega}{2\pi}|\hat{g}(\omega)|^2\Big]\Big[\frac{1}{(2\pi)^2}\int_{\mathbb{R}^2} \mathrm{d}\boldsymbol{\zeta}\exp\big(i\boldsymbol{\zeta}\cdot\boldsymbol{x}\big)\exp\Big(\frac{k_o^2}{4}\int_{z_{\mathrm{a}}}^{z_{\mathrm{b}}} C\big(\boldsymbol{\zeta}\frac{z}{k_o}\big) - C(\boldsymbol{0})\mathrm{d}z\Big)\Big], \tag{115}$$

where $k_o = k(\omega_o)$. The mean imaging function has the same resolution properties as the ones presented in Section 5.

The second-order moment of the imaging function is

$$\begin{aligned}
&\mathbb{E}\big[\mathcal{I}(\boldsymbol{x})^2\big]\\
=&\frac{1}{(2\pi z_2)^4}\iint_{\mathbb{R}\times\mathbb{R}} \frac{\mathrm{d}\omega_1\mathrm{d}\omega_2}{(2\pi)^2}k(\omega_1)^2k(\omega_2)^2\iint_{\mathbb{R}^2\times\mathbb{R}^2\times\mathbb{R}^2\times\mathbb{R}^2} \mathrm{d}\boldsymbol{x}_1\mathrm{d}\boldsymbol{x}_2\mathrm{d}\boldsymbol{y}_1\mathrm{d}\boldsymbol{y}_2\\
&\times\mathbb{E}\Big[u\big(\omega_1,\boldsymbol{x}_1,z_1\big)u\big(\omega_2,\boldsymbol{x}_2,z_1\big)\overline{u\big(\omega_1,\boldsymbol{y}_1,z_1\big)u\big(\omega_2,\boldsymbol{y}_2,z_1\big)}\Big]\\
&\times\exp\Big(-\frac{ik(\omega_1)}{2L}\big[|\boldsymbol{x}_1|^2-|\boldsymbol{y}_1|^2\big]-\frac{ik(\omega_2)}{2L}\big[|\boldsymbol{x}_2|^2-|\boldsymbol{y}_2|^2\big]\Big)\\
&\times\exp\Big(\frac{ik(\omega_1)}{2z_2}\big[|\boldsymbol{x}_1-\boldsymbol{x}|^2-|\boldsymbol{y}_1-\boldsymbol{x}|^2\big]+\frac{ik(\omega_2)}{2z_2}\big[|\boldsymbol{x}_2-\boldsymbol{x}|^2-|\boldsymbol{y}_2-\boldsymbol{x}|^2\big]\Big).
\end{aligned} \tag{116}$$

We introduce the special Fourier transform of the fourth-order moment defined by:

$$\hat{\mathcal{M}}_2\big(\omega_1,\omega_2,\boldsymbol{\xi}_1,\boldsymbol{\xi}_2,\boldsymbol{\zeta}_1,\boldsymbol{\zeta}_2,z\big)$$

$$= \iint_{\mathbb{R}^2\times\mathbb{R}^2\times\mathbb{R}^2\times\mathbb{R}^2} \mathbb{E}\Big[u\big(\omega_1,\boldsymbol{x}_1,z\big)u\big(\omega_2,\boldsymbol{x}_2,z\big)\overline{u\big(\omega_1,\boldsymbol{y}_1,z\big)u\big(\omega_2,\boldsymbol{y}_2,z\big)}\Big]$$
$$\times \exp\big(-i\boldsymbol{q}_1\cdot\boldsymbol{\xi}_1 - i\boldsymbol{r}_1\cdot\boldsymbol{\zeta}_1 - i\boldsymbol{q}_2\cdot\boldsymbol{\xi}_2 - i\boldsymbol{r}_2\cdot\boldsymbol{\zeta}_2\big)\mathrm{d}\boldsymbol{q}_1\mathrm{d}\boldsymbol{q}_2\mathrm{d}\boldsymbol{r}_1\mathrm{d}\boldsymbol{r}_2, \tag{117}$$

with the four points $\boldsymbol{x}_1,\boldsymbol{x}_2,\boldsymbol{y}_1,\boldsymbol{y}_2$ expressed in terms of $\boldsymbol{q}_1,\boldsymbol{q}_2,\boldsymbol{r}_1,\boldsymbol{r}_2$ as in (81-82). If (45) holds true, then the second-order moment of the imaging function can be written as

$$\mathbb{E}\big[\mathcal{I}(\boldsymbol{x})^2\big]$$
$$= \frac{1}{(2\pi)^8}\Big(\frac{z_1}{z_2}\Big)^4 \iint_{\mathbb{R}\times\mathbb{R}} \frac{\mathrm{d}\omega_1\mathrm{d}\omega_2}{(2\pi)^2} \iint_{\mathbb{R}^2\times\mathbb{R}^2\times\mathbb{R}^2\times\mathbb{R}^2} \mathrm{d}\boldsymbol{\xi}_1\mathrm{d}\boldsymbol{\xi}_2\mathrm{d}\boldsymbol{\zeta}_1\mathrm{d}\boldsymbol{\zeta}_2$$
$$\times \hat{\mathcal{M}}_2\big(\omega_1,\omega_2,\boldsymbol{\xi}_1,\boldsymbol{\xi}_2,\boldsymbol{\zeta}_1,\boldsymbol{\zeta}_2,z_1\big)\exp\big(2i\boldsymbol{\zeta}_1\cdot(-\frac{z_1}{z_2}\boldsymbol{x})\big)$$
$$\times \exp\Big(\frac{iz_1}{2k(\omega_1)}(\boldsymbol{\zeta}_1+\boldsymbol{\zeta}_2)\cdot(\boldsymbol{\xi}_1+\boldsymbol{\xi}_2) + \frac{iz_1}{2k(\omega_2)}(\boldsymbol{\zeta}_1-\boldsymbol{\zeta}_2)\cdot(\boldsymbol{\xi}_1-\boldsymbol{\xi}_2)\Big). \tag{118}$$

This expression shows that it is necessary to study the fourth-order moment of the transmitted field at two different frequencies.

8.1. **The two-frequency fourth-order moment of the wave field.** Let us consider two frequencies ω_1,ω_2. We consider the fourth-order moment

$$M_2(\boldsymbol{x}_1,\boldsymbol{x}_2,\boldsymbol{y}_1,\boldsymbol{y}_2,z) = \frac{\mathbb{E}\Big[u\big(\omega_1,\boldsymbol{x}_1,z\big)u\big(\omega_2,\boldsymbol{x}_2,z\big)\overline{u\big(\omega_1,\boldsymbol{y}_1,z\big)u\big(\omega_2,\boldsymbol{y}_2,z\big)}\Big]}{|\hat{g}(\omega_1)|^2|\hat{g}(\omega_2)|^2}. \tag{119}$$

It satisfies

$$\partial_z M_2 = \frac{ic_o}{2}\Big(\frac{1}{\omega_1}\Delta_{\boldsymbol{x}_1} + \frac{1}{\omega_2}\Delta_{\boldsymbol{x}_2} - \frac{1}{\omega_1}\Delta_{\boldsymbol{y}_1} - \frac{1}{\omega_2}\Delta_{\boldsymbol{y}_2}\Big)M_2$$
$$+ \frac{1}{4c_o^2}U_2\big(\boldsymbol{x}_1,\boldsymbol{x}_2,\boldsymbol{y}_1,\boldsymbol{y}_2;\omega_1,\omega_2\big)\mathbf{1}_{(z_{\mathrm{a}},z_{\mathrm{b}})}(z)M_2, \tag{120}$$

with the generalized potential

$$U_2\big(\boldsymbol{x}_1,\boldsymbol{x}_2,\boldsymbol{y}_1,\boldsymbol{y}_2;\omega_1,\omega_2\big) = \omega_1^2C(\boldsymbol{x}_1-\boldsymbol{y}_1) + \omega_1\omega_2C(\boldsymbol{x}_1-\boldsymbol{y}_2) + \omega_1\omega_2C(\boldsymbol{x}_2-\boldsymbol{y}_1)$$
$$+ \omega_2^2C(\boldsymbol{x}_2-\boldsymbol{y}_2) - \omega_1\omega_2C(\boldsymbol{x}_1-\boldsymbol{x}_2) - \omega_1\omega_2C(\boldsymbol{y}_1-\boldsymbol{y}_2)$$
$$- (\omega_1^2+\omega_2^2)C(\mathbf{0}), \tag{121}$$

and it starts from $M_2(\boldsymbol{x}_1,\boldsymbol{x}_2,\boldsymbol{y}_1,\boldsymbol{y}_2,z=0) = \exp\Big(-\frac{|\boldsymbol{x}_1|^2+|\boldsymbol{y}_1|^2+|\boldsymbol{x}_2|+|\boldsymbol{y}_2|^2}{2r_o^2}\Big)$.

We again consider the scintillation regime, that is, we assume that the radius of the initial condition (source) is much larger than the correlation radius of the random medium. We introduce a small dimensionless parameter ε in order to model this scaling regime as in (87). We also assume that the bandwidth is much smaller than the central frequency:

$$B \to \varepsilon B. \tag{122}$$

Accordingly we parameterize the two frequencies ω_1 and ω_2 as follows:

$$\omega_1 = \omega_o + \varepsilon\omega + \varepsilon\Omega, \qquad \omega_2 = \omega_o + \varepsilon\omega - \varepsilon\Omega. \tag{123}$$

We parameterize the four points $\boldsymbol{x}_1,\boldsymbol{x}_2,\boldsymbol{y}_1,\boldsymbol{y}_2$ in (120) as in (81-82) and consider a propagation distance of the form z/ε, moreover, we denote by M_2^ε the function

M_2 expressed in the variables $(\boldsymbol{q}_1, \boldsymbol{q}_2, \boldsymbol{r}_1, \boldsymbol{r}_2, z/\varepsilon)$. The function M_2^ε satisfies the equation:

$$\begin{aligned}\partial_z M_2^\varepsilon =& \frac{i}{k_o\varepsilon}\big(\nabla_{\boldsymbol{r}_1}\cdot\nabla_{\boldsymbol{q}_1}+\nabla_{\boldsymbol{r}_2}\cdot\nabla_{\boldsymbol{q}_2}\big)M_2^\varepsilon - \frac{i\omega}{k_o\omega_o}\big(\nabla_{\boldsymbol{r}_1}\cdot\nabla_{\boldsymbol{q}_1}+\nabla_{\boldsymbol{r}_2}\cdot\nabla_{\boldsymbol{q}_2}\big)M_2^\varepsilon \\ & - \frac{i\Omega}{k_o\omega_o}\big(\nabla_{\boldsymbol{r}_1}\cdot\nabla_{\boldsymbol{q}_2}+\nabla_{\boldsymbol{r}_2}\cdot\nabla_{\boldsymbol{q}_1}\big)M_2^\varepsilon + \frac{k_o^2}{4}\mathcal{U}_2(\boldsymbol{q}_1,\boldsymbol{q}_2,\boldsymbol{r}_1,\boldsymbol{r}_2)\mathbf{1}_{(z_{\rm a},z_{\rm b})}(z)M_2^\varepsilon,\end{aligned} \tag{124}$$

with the generalized potential $\mathcal{U}_2$ defined by (89) and where we have not written terms of order ε. The initial condition for Eq. (124) is

$$M_2^\varepsilon(\boldsymbol{q}_1,\boldsymbol{q}_2,\boldsymbol{r}_1,\boldsymbol{r}_2,z=0)=\exp\Big(-\varepsilon^2\frac{|\boldsymbol{r}_1|^2+|\boldsymbol{r}_2|^2}{2r_o^2}-\varepsilon^2\frac{|\boldsymbol{q}_1|^2+|\boldsymbol{q}_2|^2}{2r_o^2}\Big).$$

The Fourier transform (in $\boldsymbol{q}_1$, $\boldsymbol{q}_2$, $\boldsymbol{r}_1$, and $\boldsymbol{r}_2$) of the fourth-order moment is defined by:

$$\begin{aligned}&\hat{M}_2^\varepsilon\big(\boldsymbol{\xi}_1,\boldsymbol{\xi}_2,\boldsymbol{\zeta}_1,\boldsymbol{\zeta}_2,\frac{z}{\varepsilon}\big)\\ =&\iint_{\mathbb{R}^2\times\mathbb{R}^2\times\mathbb{R}^2\times\mathbb{R}^2} M_2^\varepsilon\big(\boldsymbol{q}_1,\boldsymbol{q}_2,\boldsymbol{r}_1,\boldsymbol{r}_2,\frac{z}{\varepsilon}\big)\\ &\times\exp\big(-i\boldsymbol{q}_1\cdot\boldsymbol{\xi}_1-i\boldsymbol{r}_1\cdot\boldsymbol{\zeta}_1-i\boldsymbol{q}_2\cdot\boldsymbol{\xi}_2-i\boldsymbol{r}_2\cdot\boldsymbol{\zeta}_2\big)\mathrm{d}\boldsymbol{r}_1\mathrm{d}\boldsymbol{r}_2\mathrm{d}\boldsymbol{q}_1\mathrm{d}\boldsymbol{q}_2.\end{aligned} \tag{125}$$

Let us absorb the rapid phase in the function

$$\widetilde{M}_2^\varepsilon\big(\boldsymbol{\xi}_1,\boldsymbol{\xi}_2,\boldsymbol{\zeta}_1,\boldsymbol{\zeta}_2,\frac{z}{\varepsilon}\big)=\hat{M}_2^\varepsilon\big(\boldsymbol{\xi}_1,\boldsymbol{\xi}_2,\boldsymbol{\zeta}_1,\boldsymbol{\zeta}_2,\frac{z}{\varepsilon}\big)\exp\Big(\frac{iz}{k_o\varepsilon}(\boldsymbol{\xi}_2\cdot\boldsymbol{\zeta}_2+\boldsymbol{\xi}_1\cdot\boldsymbol{\zeta}_1)\Big). \tag{126}$$

In the scintillation regime the rescaled function $\widetilde{M}_2^\varepsilon$ satisfies the equation with fast phases

$$\begin{aligned}\partial_z\widetilde{M}_2^\varepsilon =& \frac{i\omega}{k_o\omega_o}(\boldsymbol{\xi}_1\cdot\boldsymbol{\zeta}_1+\boldsymbol{\xi}_2\cdot\boldsymbol{\zeta}_2)\widetilde{M}_2^\varepsilon+\frac{i\Omega}{k_o\omega_o}(\boldsymbol{\xi}_1\cdot\boldsymbol{\zeta}_2+\boldsymbol{\xi}_2\cdot\boldsymbol{\zeta}_1)\widetilde{M}_2^\varepsilon\\ &+\frac{k_o^2}{4(2\pi)^2}\mathbf{1}_{(z_{\rm a},z_{\rm b})}(z)\int_{\mathbb{R}^2}\hat{C}(\boldsymbol{k})\Big[-2\widetilde{M}_2^\varepsilon(\boldsymbol{\xi}_1,\boldsymbol{\xi}_2,\boldsymbol{\zeta}_1,\boldsymbol{\zeta}_2)\\ &+\widetilde{M}_2^\varepsilon(\boldsymbol{\xi}_1-\boldsymbol{k},\boldsymbol{\xi}_2-\boldsymbol{k},\boldsymbol{\zeta}_1,\boldsymbol{\zeta}_2)e^{i\frac{z}{\varepsilon k_o}\boldsymbol{k}\cdot(\boldsymbol{\zeta}_2+\boldsymbol{\zeta}_1)}\\ &+\widetilde{M}_2^\varepsilon(\boldsymbol{\xi}_1-\boldsymbol{k},\boldsymbol{\xi}_2,\boldsymbol{\zeta}_1,\boldsymbol{\zeta}_2-\boldsymbol{k})e^{i\frac{z}{\varepsilon k_o}\boldsymbol{k}\cdot(\boldsymbol{\xi}_2+\boldsymbol{\zeta}_1)}\\ &+\widetilde{M}_2^\varepsilon(\boldsymbol{\xi}_1+\boldsymbol{k},\boldsymbol{\xi}_2-\boldsymbol{k},\boldsymbol{\zeta}_1,\boldsymbol{\zeta}_2)e^{i\frac{z}{\varepsilon k_o}\boldsymbol{k}\cdot(\boldsymbol{\zeta}_2-\boldsymbol{\zeta}_1)}\\ &+\widetilde{M}_2^\varepsilon(\boldsymbol{\xi}_1+\boldsymbol{k},\boldsymbol{\xi}_2,\boldsymbol{\zeta}_1,\boldsymbol{\zeta}_2-\boldsymbol{k})e^{i\frac{z}{\varepsilon k_o}\boldsymbol{k}\cdot(\boldsymbol{\xi}_2-\boldsymbol{\zeta}_1)}\\ &-\widetilde{M}_2^\varepsilon(\boldsymbol{\xi}_1,\boldsymbol{\xi}_2-\boldsymbol{k},\boldsymbol{\zeta}_1,\boldsymbol{\zeta}_2-\boldsymbol{k})e^{i\frac{z}{\varepsilon k_o}(\boldsymbol{k}\cdot(\boldsymbol{\zeta}_2+\boldsymbol{\xi}_2)-|\boldsymbol{k}|^2)}\\ &-\widetilde{M}_2^\varepsilon(\boldsymbol{\xi}_1,\boldsymbol{\xi}_2-\boldsymbol{k},\boldsymbol{\zeta}_1,\boldsymbol{\zeta}_2+\boldsymbol{k})e^{i\frac{z}{\varepsilon k_o}(\boldsymbol{k}\cdot(\boldsymbol{\zeta}_2-\boldsymbol{\xi}_2)+|\boldsymbol{k}|^2)}\Big]\mathrm{d}\boldsymbol{k},\end{aligned} \tag{127}$$

starting from $\widetilde{M}_2^\varepsilon(\boldsymbol{\xi}_1,\boldsymbol{\xi}_2,\boldsymbol{\zeta}_1,\boldsymbol{\zeta}_2,z=0)=(2\pi)^8\phi_{r_o}^\varepsilon(\boldsymbol{\xi}_1)\phi_{r_o}^\varepsilon(\boldsymbol{\xi}_2)\phi_{r_o}^\varepsilon(\boldsymbol{\zeta}_1)\phi_{r_o}^\varepsilon(\boldsymbol{\zeta}_2)$, where $\phi_{r_o}^\varepsilon$ is defined by (93). The following result shows that $\widetilde{M}_2^\varepsilon$ exhibits a multi-scale behavior as $\varepsilon\to 0$, with some components evolving at the scale ε and some components evolving at the scale 1.

Proposition 8. *The function $\widetilde{M}_2^\varepsilon(\boldsymbol{\xi}_1,\boldsymbol{\xi}_2,\boldsymbol{\zeta}_1,\boldsymbol{\zeta}_2,z/\varepsilon)$ can be expanded as*

$$\widetilde{M}_2^\varepsilon\big(\boldsymbol{\xi}_1,\boldsymbol{\xi}_2,\boldsymbol{\zeta}_1,\boldsymbol{\zeta}_2,\frac{z}{\varepsilon}\big)$$

$$
\begin{aligned}
= \quad & K(z)^2\phi^\varepsilon_{r_o}(\boldsymbol{\xi}_1)\phi^\varepsilon_{r_o}(\boldsymbol{\xi}_2)\phi^\varepsilon_{r_o}(\boldsymbol{\zeta}_1)\phi^\varepsilon_{r_o}(\boldsymbol{\zeta}_2)\\
&+\frac{K(z)}{2}\phi^\varepsilon_{r_o}\big(\frac{\boldsymbol{\xi}_1-\boldsymbol{\xi}_2}{\sqrt{2}}\big)\phi^\varepsilon_{r_o}(\boldsymbol{\zeta}_1)\phi^\varepsilon_{r_o}(\boldsymbol{\zeta}_2)A\big(z,\frac{\boldsymbol{\xi}_2+\boldsymbol{\xi}_1}{2},\frac{\boldsymbol{\zeta}_2+\boldsymbol{\zeta}_1}{\varepsilon},0\big)\\
&+\frac{K(z)}{2}\phi^\varepsilon_{r_o}\big(\frac{\boldsymbol{\xi}_1+\boldsymbol{\xi}_2}{\sqrt{2}}\big)\phi^\varepsilon_{r_o}(\boldsymbol{\zeta}_1)\phi^\varepsilon_{r_o}(\boldsymbol{\zeta}_2)A\big(z,\frac{\boldsymbol{\xi}_2-\boldsymbol{\xi}_1}{2},\frac{\boldsymbol{\zeta}_2-\boldsymbol{\zeta}_1}{\varepsilon},0\big)\\
&+\frac{K(z)}{2}\phi^\varepsilon_{r_o}\big(\frac{\boldsymbol{\xi}_1-\boldsymbol{\zeta}_2}{\sqrt{2}}\big)\phi^\varepsilon_{r_o}(\boldsymbol{\zeta}_1)\phi^\varepsilon_{r_o}(\boldsymbol{\xi}_2)A\big(z,\frac{\boldsymbol{\zeta}_2+\boldsymbol{\xi}_1}{2},\frac{\boldsymbol{\xi}_2+\boldsymbol{\zeta}_1}{\varepsilon},\Omega\big)\\
&+\frac{K(z)}{2}\phi^\varepsilon_{r_o}\big(\frac{\boldsymbol{\xi}_1+\boldsymbol{\zeta}_2}{\sqrt{2}}\big)\phi^\varepsilon_{r_o}(\boldsymbol{\zeta}_1)\phi^\varepsilon_{r_o}(\boldsymbol{\xi}_2)A\big(z,\frac{\boldsymbol{\zeta}_2-\boldsymbol{\xi}_1}{2},\frac{\boldsymbol{\xi}_2-\boldsymbol{\zeta}_1}{\varepsilon},-\Omega\big)\\
&+\frac{1}{4}\phi^\varepsilon_{r_o}(\boldsymbol{\zeta}_1)\phi^\varepsilon_{r_o}(\boldsymbol{\zeta}_2)A\big(z,\frac{\boldsymbol{\xi}_2+\boldsymbol{\xi}_1}{2},\frac{\boldsymbol{\zeta}_2+\boldsymbol{\zeta}_1}{\varepsilon},0\big)A\big(z,\frac{\boldsymbol{\xi}_2-\boldsymbol{\xi}_1}{2},\frac{\boldsymbol{\zeta}_2-\boldsymbol{\zeta}_1}{\varepsilon},0\big)\\
&+\frac{1}{4}\phi^\varepsilon_{r_o}(\boldsymbol{\zeta}_1)\phi^\varepsilon_{r_o}(\boldsymbol{\xi}_2)A\big(z,\frac{\boldsymbol{\zeta}_2+\boldsymbol{\xi}_1}{2},\frac{\boldsymbol{\xi}_2+\boldsymbol{\zeta}_1}{\varepsilon},\Omega\big)A\big(z,\frac{\boldsymbol{\zeta}_2-\boldsymbol{\xi}_1}{2},\frac{\boldsymbol{\xi}_2-\boldsymbol{\zeta}_1}{\varepsilon},-\Omega\big)\\
&+R_2^\varepsilon(z,\boldsymbol{\xi}_1,\boldsymbol{\xi}_2,\boldsymbol{\zeta}_1,\boldsymbol{\zeta}_2),
\end{aligned}
\tag{128}
$$

where the function K is defined by (95), the function $(z,\boldsymbol{\xi})\mapsto A(z,\boldsymbol{\xi},\boldsymbol{\zeta},\Omega)$ is the solution of (96) starting from $A(z=0,\boldsymbol{\xi},\boldsymbol{\zeta},\Omega)=0$, and the function R_2^ε satisfies (97).

This result is an extension of Proposition 6 in which the case $\omega=\Omega=0$ is addressed. It shows that, if we deal with an integral of $\widetilde{M}_2^\varepsilon$ against a bounded function, then we can replace $\widetilde{M}_2^\varepsilon$ by the right-hand side of (128) without the R_2^ε term up to a negligible error when ε is small.

8.2. **The second-order moment of the optical imaging function in the broadband case.** We consider the scintillation regime, that is, we assume that the radius of the initial condition is much larger than the correlation radius of the random medium and that the bandwidth is much smaller than the central frequency. We, therefore, introduce a small dimensionless parameter ε in order to model this scaling regime as in (87)-(122).

Proposition 9. *When $\varepsilon\to 0$, the mean optical imaging function is*

$$
\begin{aligned}
&\mathbb{E}\big[\mathcal{I}\big(\frac{\boldsymbol{x}}{\varepsilon}\big)\big]\\
=&\Big[\int_{\mathbb{R}}\frac{\mathrm{d}s}{2\pi}|\hat g_0(s)|^2\Big]\Big(\frac{z_1}{z_2}\Big)^2\\
&\times\Big[\frac{r_o^2}{4\pi}\int_{\mathbb{R}^2}\mathrm{d}\boldsymbol{\zeta}\exp\Big(i\boldsymbol{\zeta}\cdot(-\frac{z_1}{z_2}\boldsymbol{x})-\frac{r_o^2|\boldsymbol{\zeta}|^2}{4}+\frac{k_o^2}{4}\int_{z_{\rm a}}^{z_{\rm b}}C\big(\boldsymbol{\zeta}\frac{z}{k_o}\big)-C(\mathbf{0})\mathrm{d}z\Big)\Big],
\end{aligned}
\tag{129}
$$

and its variance is

$$
\begin{aligned}
&\mathrm{Var}\big(\mathcal{I}(\frac{\boldsymbol{x}}{\varepsilon})\big)\\
=&\frac{1}{(2\pi)^8}\Big(\frac{z_1}{z_2}\Big)^4\int_{\mathbb{R}}\frac{\mathrm{d}\Omega}{2\pi B}\Big[\int_{\mathbb{R}}\frac{\mathrm{d}\omega}{4\pi B}\Big|\hat g_0\Big(\frac{\omega+\Omega}{B}\Big)\Big|^2\Big|\hat g_0\Big(\frac{\omega-\Omega}{B}\Big)\Big|^2\Big]\\
&\times\iint_{\mathbb{R}^2\times\mathbb{R}^2}\mathrm{d}\boldsymbol{\alpha}\mathrm{d}\boldsymbol{\beta}\exp\Big(i(\boldsymbol{\alpha}-\boldsymbol{\beta})\cdot(-\frac{z_1}{z_2}\boldsymbol{x})\Big)\phi^1_{\frac{r_o}{\sqrt{2}}}(\boldsymbol{\alpha})\phi^1_{\frac{r_o}{\sqrt{2}}}(\boldsymbol{\beta})\\
&\times\Big\{K(z_1)E\big(z_1,\boldsymbol{\alpha},\Omega\big)+K(z_1)E\big(z_1,\boldsymbol{\beta},-\Omega\big)+E\big(z_1,\boldsymbol{\alpha},\Omega\big)E\big(z_1,\boldsymbol{\beta},-\Omega\big)\Big\},
\end{aligned}
\tag{130}
$$

with

$$E(z_1,\boldsymbol{\zeta},\Omega)=\int_{\mathbb{R}^2}\mathrm{d}\boldsymbol{\xi}A(z_1,\boldsymbol{\xi},\boldsymbol{\zeta},\Omega)\exp\big(-i\frac{|\boldsymbol{\xi}|^2\Omega z_1}{k_o\omega_o}\big). \tag{131}$$

Proof. First, the expression of the mean of the optical imaging function follows from (71) in the regime (87)-(122). Second, we find that the second-order moment of the imaging function is

$$\begin{aligned}
&\mathbb{E}\big[\mathcal{I}(\frac{\boldsymbol{x}}{\varepsilon})^2\big]\\
=&\frac{1}{(2\pi)^8}\Big(\frac{z_1}{z_2}\Big)^4\iint_{\mathbb{R}\times\mathbb{R}}\frac{\mathrm{d}\omega\mathrm{d}\Omega}{2(2\pi)^2B^2}\Big|\hat{g}_0\Big(\frac{\omega+\Omega}{B}\Big)\Big|^2\Big|\hat{g}_0\Big(\frac{\omega-\Omega}{B}\Big)\Big|^2\\
&\times\int_{\mathbb{R}^2}\mathrm{d}\boldsymbol{\zeta}_1\exp\big(2i\boldsymbol{\zeta}_1\cdot(-\frac{z_1}{z_2}\boldsymbol{x})\big)\phi^1_{r_o}(\boldsymbol{\zeta}_1)\Big\{K(z_1)^2\\
&+K(z_1)\iint_{\mathbb{R}^2\times\mathbb{R}^2}\mathrm{d}\boldsymbol{\zeta}_2\mathrm{d}\boldsymbol{\xi}_2\phi^1_{r_o}(\boldsymbol{\zeta}_2)\big[A(z_1,\boldsymbol{\xi}_2,\boldsymbol{\zeta}_2+\boldsymbol{\zeta}_1,0)+A(z_1,\boldsymbol{\xi}_2,\boldsymbol{\zeta}_2-\boldsymbol{\zeta}_1,0)\big]\\
&+K(z_1)\iint_{\mathbb{R}^2\times\mathbb{R}^2}\mathrm{d}\boldsymbol{\zeta}_2\mathrm{d}\boldsymbol{\xi}_2\phi^1_{r_o}(\boldsymbol{\xi}_2)A(z_1,\boldsymbol{\zeta}_2,\boldsymbol{\xi}_2+\boldsymbol{\zeta}_1,\Omega)\exp\big(-i\frac{|\boldsymbol{\zeta}_2|^2\Omega z_1}{k_o\omega_o}\big)\\
&+K(z_1)\iint_{\mathbb{R}^2\times\mathbb{R}^2}\mathrm{d}\boldsymbol{\zeta}_2\mathrm{d}\boldsymbol{\xi}_2\phi^1_{r_o}(\boldsymbol{\xi}_2)A(z_1,\boldsymbol{\zeta}_2,\boldsymbol{\xi}_2-\boldsymbol{\zeta}_1,-\Omega)\exp\big(i\frac{|\boldsymbol{\zeta}_2|^2\Omega z_1}{k_o\omega_o}\big)\\
&+\frac{1}{4}\iint_{\mathbb{R}^2\times\mathbb{R}^2\times\mathbb{R}^2}\mathrm{d}\boldsymbol{\zeta}_2\mathrm{d}\boldsymbol{\xi}_1\mathrm{d}\boldsymbol{\xi}_2\phi^1_{r_o}(\boldsymbol{\zeta}_2)A(z_1,\frac{\boldsymbol{\xi}_2+\boldsymbol{\xi}_1}{2},\boldsymbol{\zeta}_2+\boldsymbol{\zeta}_1,0)\\
&\qquad\qquad\times A(z_1,\frac{\boldsymbol{\xi}_2-\boldsymbol{\xi}_1}{2},\boldsymbol{\zeta}_2-\boldsymbol{\zeta}_1,0)\\
&+\frac{1}{4}\iint_{\mathbb{R}^2\times\mathbb{R}^2\times\mathbb{R}^2}\mathrm{d}\boldsymbol{\zeta}_2\mathrm{d}\boldsymbol{\xi}_1\mathrm{d}\boldsymbol{\xi}_2\phi^1_{r_o}(\boldsymbol{\xi}_2)A(z_1,\frac{\boldsymbol{\zeta}_2+\boldsymbol{\xi}_1}{2},\boldsymbol{\xi}_2+\boldsymbol{\zeta}_1,\Omega)\\
&\qquad\qquad\times A(z_1,\frac{\boldsymbol{\zeta}_2-\boldsymbol{\xi}_1}{2},\boldsymbol{\xi}_2-\boldsymbol{\zeta}_1,-\Omega)\exp\big(-i\frac{\boldsymbol{\zeta}_2\cdot\boldsymbol{\xi}_1\Omega z_1}{k_o\omega_o}\big)\Big\}.
\end{aligned}$$

Therefore, we can write

$$\begin{aligned}
&\mathrm{Var}\big(\mathcal{I}(\frac{\boldsymbol{x}}{\varepsilon})\big)=\frac{1}{(2\pi)^8}\Big(\frac{z_1}{z_2}\Big)^4\iint_{\mathbb{R}\times\mathbb{R}}\frac{\mathrm{d}\omega\mathrm{d}\Omega}{2(2\pi)^2B^2}\Big|\hat{g}_0\Big(\frac{\omega+\Omega}{B}\Big)\Big|^2\Big|\hat{g}_0\Big(\frac{\omega-\Omega}{B}\Big)\Big|^2\\
&\times\int_{\mathbb{R}^2}\mathrm{d}\boldsymbol{\zeta}_1\exp\big(2i\boldsymbol{\zeta}_1\cdot(-\frac{z_1}{z_2}\boldsymbol{x})\big)\phi^1_{r_o}(\boldsymbol{\zeta}_1)\\
&\times\Big\{K(z_1)\iint_{\mathbb{R}^2\times\mathbb{R}^2}\mathrm{d}\boldsymbol{\zeta}_2\mathrm{d}\boldsymbol{\xi}_2\phi^1_{r_o}(\boldsymbol{\zeta}_2)A(z_1,\boldsymbol{\xi}_2,\boldsymbol{\zeta}_2+\boldsymbol{\zeta}_1,\Omega)\exp\big(-i\frac{|\boldsymbol{\xi}_2|^2\Omega z_1}{k_o\omega_o}\big)\\
&\quad+K(z_1)\iint_{\mathbb{R}^2\times\mathbb{R}^2}\mathrm{d}\boldsymbol{\zeta}_2\mathrm{d}\boldsymbol{\xi}_2\phi^1_{r_o}(\boldsymbol{\zeta}_2)A(z_1,\boldsymbol{\xi}_2,\boldsymbol{\zeta}_2-\boldsymbol{\zeta}_1,-\Omega)\exp\big(i\frac{|\boldsymbol{\xi}_2|^2\Omega z_1}{k_o\omega_o}\big)\\
&\quad+\frac{1}{4}\iint_{\mathbb{R}^2\times\mathbb{R}^2\times\mathbb{R}^2}\mathrm{d}\boldsymbol{\zeta}_2\mathrm{d}\boldsymbol{\xi}_1\mathrm{d}\boldsymbol{\xi}_2\phi^1_{r_o}(\boldsymbol{\zeta}_2)A(z_1,\frac{\boldsymbol{\xi}_2+\boldsymbol{\xi}_1}{2},\boldsymbol{\zeta}_2+\boldsymbol{\zeta}_1,\Omega)\\
&\qquad\qquad\times A(z_1,\frac{\boldsymbol{\xi}_2-\boldsymbol{\xi}_1}{2},\boldsymbol{\zeta}_2-\boldsymbol{\zeta}_1,-\Omega)\exp\big(-i\frac{\boldsymbol{\xi}_2\cdot\boldsymbol{\xi}_1\Omega z_1}{k_o\omega_o}\big)\Big\},
\end{aligned}$$

which gives the expression (130) of the variance of the imaging function. □

The expression (129) of the mean imaging function shows that the bandwidth does not affect the resolution in this regime. The variance of the imaging function is given by the expression (130), which is exact but quite complicated. This expression

can be simplified in the strongly scattering regime and we address this problem in the next subsection.

8.3. **The second-order moment of the optical imaging function in the broadband case and in the strongly scattering regime.** In the strongly scattering regime, when $z_{\rm b}-z_{\rm a}\gg\ell_{\rm sca}$ and the random medium is smooth so that $C(\boldsymbol{x})$ can be expanded as (38), then the mean optical imaging function is

$$\mathbb{E}\big[\mathcal{I}\big(\frac{\boldsymbol{x}}{\varepsilon}\big)\big]=\Big(\frac{z_1}{z_2}\Big)^2\Big[\int_{\mathbb{R}}\frac{\mathrm{d}s}{2\pi}|\hat{g}_0(s)|^2\Big]\frac{1}{1+\frac{z_{\rm b}^3-z_{\rm a}^3}{3r_o^2\ell_{\rm par}}}\exp\Big(-\frac{|-\frac{z_1}{z_2}\boldsymbol{x}|^2}{r_o^2+\frac{z_{\rm b}^3-z_{\rm a}^3}{3\ell_{\rm par}}}\Big), \tag{132}$$

while the function A solution of (96) can be approximated by the solution of the parabolic partial differential equation

$$\partial_z A_{\rm s}=\frac{i\Omega}{k_o\omega_o}|\boldsymbol{\xi}|^2A_{\rm s}+\frac{k_o^2}{4\ell_{\rm par}}\mathbf{1}_{(z_{\rm a},z_{\rm b})}(z)\Big[\Delta_{\boldsymbol{\xi}}A_{\rm s}-\frac{z^2}{k_o^2}|\boldsymbol{\zeta}|^2A_{\rm s}-2i\frac{z}{k_o}\boldsymbol{\zeta}\cdot\nabla_{\boldsymbol{\xi}}A_{\rm s}\Big], \tag{133}$$

starting from $A_{\rm s}(z=0,\boldsymbol{\xi},\boldsymbol{\zeta},\Omega)=(2\pi)^4\delta(\boldsymbol{\xi})$. If we consider the partial inverse Fourier transform

$$\hat{A}_{\rm s}(z,\boldsymbol{x},\boldsymbol{\zeta},\Omega)=\frac{1}{(2\pi)^2}\int_{\mathbb{R}^2}A_{\rm s}(z,\boldsymbol{\xi},\boldsymbol{\zeta},\Omega)\exp(i\boldsymbol{\xi}\cdot\boldsymbol{x})\mathrm{d}\boldsymbol{\xi}. \tag{134}$$

then it is solution of

$$\partial_z\hat{A}_{\rm s}=-\frac{i\Omega}{k_o\omega_o}\Delta_{\boldsymbol{x}}\hat{A}_{\rm s}-\frac{k_o^2}{4\ell_{\rm par}}\mathbf{1}_{(z_{\rm a},z_{\rm b})}(z)\Big[|\boldsymbol{x}|^2+\frac{z^2}{k_o^2}|\boldsymbol{\zeta}|^2+2\frac{z}{k_o}\boldsymbol{\zeta}\cdot\boldsymbol{x}\Big]\hat{A}_{\rm s}, \tag{135}$$

starting from $\hat{A}_{\rm s}(z=0,\boldsymbol{x},\boldsymbol{\zeta},\Omega)=(2\pi)^2$. The solution has the form

$$\hat{A}_{\rm s}(z,\boldsymbol{x},\boldsymbol{\zeta},\Omega)=(2\pi)^2\exp\big[-a_\Omega(z)-b_\Omega(z)|\boldsymbol{x}|^2-c_\Omega(z)\boldsymbol{x}\cdot\boldsymbol{\zeta}-d_\Omega(z)|\boldsymbol{\zeta}|^2\big], \tag{136}$$

where $(a_\Omega,b_\Omega,c_\Omega,d_\Omega)$ is the solution of the system of ordinary differential equations:

$$\begin{aligned}
\frac{\mathrm{d}a_\Omega}{\mathrm{d}z}&=-i\frac{4\Omega}{k_o\omega_o}b_\Omega,\\
\frac{\mathrm{d}b_\Omega}{\mathrm{d}z}&=\frac{k_o^2}{4\ell_{\rm par}}\mathbf{1}_{(z_{\rm a},z_{\rm b})}(z)+i\frac{4\Omega}{k_o\omega_o}b_\Omega^2,\\
\frac{\mathrm{d}c_\Omega}{\mathrm{d}z}&=\frac{k_oz}{2\ell_{\rm par}}\mathbf{1}_{(z_{\rm a},z_{\rm b})}(z)+i\frac{4\Omega}{k_o\omega_o}b_\Omega c_\Omega,\\
\frac{\mathrm{d}d_\Omega}{\mathrm{d}z}&=\frac{z^2}{4\ell_{\rm par}}\mathbf{1}_{(z_{\rm a},z_{\rm b})}(z)+i\frac{\Omega}{k_o\omega_o}c_\Omega^2,
\end{aligned}$$

starting from $(a_\Omega,b_\Omega,c_\Omega,d_\Omega)(z=0)=(0,0,0,0)$. We have $(a_{-\Omega},b_{-\Omega},c_{-\Omega},d_{-\Omega})(z)=(\overline{a_\Omega},\overline{b_\Omega},\overline{c_\Omega},\overline{d_\Omega})(z)$ and by solving the system, we obtain

$$a_\Omega(z_{\rm b})=\Psi_a\Big(\sqrt{\frac{\Omega}{c_o\ell_{\rm par}}}(z_{\rm b}-z_{\rm a})\Big), \tag{137}$$

$$b_\Omega(z_{\rm b})=\frac{k_o^2(z_{\rm b}-z_{\rm a})}{4\ell_{\rm par}}\Psi_b\Big(\sqrt{\frac{\Omega}{c_o\ell_{\rm par}}}(z_{\rm b}-z_{\rm a})\Big), \tag{138}$$

$$c_\Omega(z_{\rm b})=\frac{k_o(z_{\rm b}-z_{\rm a})^2}{4\ell_{\rm par}}\Psi_c\Big(\sqrt{\frac{\Omega}{c_o\ell_{\rm par}}}(z_{\rm b}-z_{\rm a})\Big), \tag{139}$$

$$d_\Omega(z_{\rm b})=\frac{(z_{\rm b}-z_{\rm a})^3}{12\ell_{\rm par}}\Psi_d\Big(\sqrt{\frac{\Omega}{c_o\ell_{\rm par}}}(z_{\rm b}-z_{\rm a})\Big), \tag{140}$$

for $\Omega \geq 0$ with the functions $\Psi_{a,b,c,d}$ defined by

$$\Psi_a(s) = \ln\Big[\cosh\big(e^{-i\frac{\pi}{4}}s\big)\Big], \tag{141}$$

$$\Psi_b(s) = \frac{\tanh(e^{-i\frac{\pi}{4}}s)}{e^{-i\frac{\pi}{4}}s}, \tag{142}$$

$$\Psi_c(s) = 2i\frac{e^{-i\frac{\pi}{4}}s\tanh(e^{-i\frac{\pi}{4}}s) - 1 + \cosh^{-1}(e^{-i\frac{\pi}{4}}s)}{s^2}, \tag{143}$$

$$\Psi_d(s) = 1 - \frac{3i}{s^3}\int_0^s \big(e^{-i\frac{\pi}{4}}s'\tanh(e^{-i\frac{\pi}{4}}s') - 1 + \cosh^{-1}(e^{-i\frac{\pi}{4}}s')\big)^2 \mathrm{d}s', \tag{144}$$

for $s \geq 0$. Finally

$$a_\Omega(z_1) = a_\Omega(z_\mathrm{b}) + \ln\Big(1 - \frac{4ib_\Omega(z_\mathrm{b})\Omega(z_1 - z_\mathrm{b})}{k_o\omega_o}\Big), \tag{145}$$

$$b_\Omega(z_1) = \frac{b_\Omega(z_\mathrm{b})}{1 - \frac{4ib_\Omega(z_\mathrm{b})\Omega(z_1-z_\mathrm{b})}{k_o\omega_o}}, \tag{146}$$

$$c_\Omega(z_1) = \frac{c_\Omega(z_\mathrm{b})}{1 - \frac{4ib_\Omega(z_\mathrm{b})\Omega(z_1-z_\mathrm{b})}{k_o\omega_o}}, \tag{147}$$

$$d_\Omega(z_1) = d_\Omega(z_\mathrm{b}) + \frac{i\Omega(z_1 - z_\mathrm{b})c_\Omega(z_\mathrm{b})^2}{k_o\omega_o - 4i\Omega(z_1 - z_\mathrm{b})b_\Omega(z_\mathrm{b})}. \tag{148}$$

We then get (with $a_\Omega, b_\Omega, c_\Omega, d_\Omega$ evaluated at z_1)

$$\begin{aligned}\mathrm{Var}\big(\mathcal{I}(\frac{\boldsymbol{x}}{\varepsilon})\big) =& \Big(\frac{z_1}{z_2}\Big)^4 \int_{\mathbb{R}} \frac{\mathrm{d}\Omega}{2\pi B}\Big[\int_{\mathbb{R}} \frac{\mathrm{d}\omega}{4\pi B}\Big|\hat g_0\Big(\frac{\omega+\Omega}{B}\Big)\Big|^2\Big|\hat g_0\Big(\frac{\omega-\Omega}{B}\Big)\Big|^2\Big]\exp\big(-2\mathrm{Re}(a_\Omega)\big) \\ &\times\Big|\frac{1}{(1+\frac{4d_\Omega}{r_o^2})(1+i\frac{4z_1\Omega b_\Omega}{k_o\omega_o})}\exp\Big(-\frac{|-\frac{z_1}{z_2}\boldsymbol{x}|^2}{r_o^2(1+\frac{4d_\Omega}{r_o^2}-\frac{4c_\Omega^2}{b_\Omega r_o^2 - i\frac{k_o\omega_o r_o^2}{4z_1\Omega}})}\Big)\Big|^2.\end{aligned} \tag{149}$$

If

$$\frac{B}{c_o\ell_{\mathrm{par}}}(z_\mathrm{b} - z_\mathrm{a})^2 \ll 1,$$

then

$$\mathrm{Var}\big(\mathcal{I}(\frac{\boldsymbol{x}}{\varepsilon})\big) = \Big(\frac{z_1}{z_2}\Big)^4\Big[\int_{\mathbb{R}}\frac{\mathrm{d}s}{2\pi}|\hat g_0(s)|^2\Big]^2\Big[\frac{1}{1+\frac{z_\mathrm{b}^3 - z_\mathrm{a}^3}{3r_o^2\ell_{\mathrm{par}}}}\exp\Big(-\frac{|-\frac{z_1}{z_2}\boldsymbol{x}|^2}{r_o^2 + \frac{z_\mathrm{b}^3 - z_\mathrm{a}^3}{3\ell_{\mathrm{par}}}}\Big)\Big]^2. \tag{150}$$

By comparing with (132) this shows that the imaging function is not stable:

$$\frac{\mathrm{Var}\big(\mathcal{I}(\frac{\boldsymbol{x}}{\varepsilon})\big)}{\mathbb{E}\big[\big(\mathcal{I}(\frac{\boldsymbol{x}}{\varepsilon})\big]^2} = 1. \tag{151}$$

If

$$\frac{B}{c_o\ell_{\mathrm{par}}}(z_\mathrm{b} - z_\mathrm{a})^2 \gg 1,$$

then

$$\begin{aligned}&\mathrm{Var}\big(\mathcal{I}(\frac{\boldsymbol{x}}{\varepsilon})\big) \\ =&\Big(\frac{z_1}{z_2}\Big)^4\Big[\int_{\mathbb{R}}\frac{\mathrm{d}s}{4\pi}\big|\hat g_0(s)\big|^4\Big]\Big[\int_{\mathbb{R}}\frac{\mathrm{d}s}{2\pi}\exp\big(-2\mathrm{Re}(a_{Bs})\big)\end{aligned}$$

$$\times \Big| \frac{1}{(1+\frac{4d_{Bs}}{r_o^2})(1+i\frac{4z_1\Omega b_{Bs}}{k_o\omega_o})} \exp\Big(-\frac{|-\frac{z_1}{z_2}\boldsymbol{x}|^2}{r_o^2(1+\frac{4d_{Bs}}{r_o^2}-\frac{4c_{Bs}^2}{b_{Bs}r_o^2-i\frac{k_o\omega_o r_o^2}{4z_1 B s}})}\Big)\Big|^2\Big]. \quad (152)$$

By comparing with (132) and by taking into account the fact that

$$\exp\big(-2\mathrm{Re}(a_{Bs})\big) = \frac{1}{1+\frac{16|b_{Bs}(z_{\rm b})|^2B^2s^2(z_1-z_{\rm b})^2}{k_o^2\omega_o^2}} \times \frac{2}{\cosh(\sqrt{\frac{2B}{c_o\ell_{\rm par}}}(z_{\rm b}-z_{\rm a})\sqrt{|s|}) + \cos(\sqrt{\frac{2B}{c_o\ell_{\rm par}}}(z_{\rm b}-z_{\rm a})\sqrt{|s|})}$$

decays as $\exp(-\sqrt{2B/(c_o\ell_{\rm par})}(z_{\rm b}-z_{\rm a})\sqrt{|s|})$, this shows that the imaging function is stable:

$$\frac{\mathrm{Var}\big(\mathcal{I}(\frac{\boldsymbol{x}}{\varepsilon})\big)}{\mathbb{E}\big[\mathcal{I}(\frac{\boldsymbol{x}}{\varepsilon})\big]^2} = O\Big(\frac{\omega_{\rm c}}{B}\Big), \qquad \omega_{\rm c} = \frac{c_o\ell_{\rm par}}{(z_{\rm b}-z_{\rm a})^2}. \quad (153)$$

To summarize, the statistical stability of the image is ensured by the source bandwidth. If the source bandwidth is larger than the coherence frequency $\omega_{\rm c}$ then the image is stable.

9. **Conclusions.** We have analyzed the shower curtain effect and found that it is an effect associated with the incoherent wave field and driven by random lateral scattering. The intensity of this lateral scattering depends on the location of the random section (the shower curtain) relative to the source. We expect that the shower curtain effect can also be observed in a wave transport regime or for a wave transmission problem through a rough interface, while it is small or even vanishes for a medium with strong lateral coherence like a randomly (quasi-)layered medium [6]. Note that optical imaging (with a lens) is less sensitive to the complex medium fluctuations than matched field imaging. We have moreover shown that for optical imaging in the strongly scattering regime the use of broadband signals is important for statistical stability and high signal-to-noise ratio. Here broadband means a broad frequency-band relative to the coherence frequency. We remark that another mechanism to obtain statistical stability is via multiple snapshots in a time-dependent medium, see for instance [11]. In this paper we have considered a coherent source and passive source imaging while recent physical experiments and numerical studies have used partly coherent sources and active imaging configurations. Such configurations will be the subject of future work in view of the tools presented here.

Acknowledgments. JG was supported by the Agence Nationale de la Recherche under Grant No. ANR-19-CE46-0007 (project ICCI) and Air Force Office of Scientific Research under grant FA9550-22-1-0176. KS was supported by the Air Force Office of Scientific Research under grant FA9550-22-1-0176 and the National Science Foundation under grant DMS-2308389.

REFERENCES

[1] L. C. Andrews and R. L. Phillips, *Laser Beam Propagation through Random Media*, SPIE, Bellingham, 2005.

[2] D. A. Dawson and G. C. Papanicolaou, A random wave process, *Appl. Math. Optim.*, **12** (1984), 97-114 .

[3] M. V. de Hoop, J. Garnier and K. Sølna, Three-dimensional random wave coupling along a boundary and an associated inverse problem, *SIAM Multiscale Model. Simul.*, **22** (2024), 39-65.

[4] I. Dror, A. Sandrov and N. S. Kopeika, Experimental investigation of the influence of the relative position of the scattering layer on image quality: The shower curtain effect, *Appl. Opt.*, **37** (1998), 6495-6499.
[5] E. Edrei and G. Scarcelli, Optical imaging through dynamic turbid media using the Fourier-domain shower-curtain effect, *Optica*, **3** (2016), 71-74.
[6] J.-P. Fouque, J. Garnier, G. Papanicolaou and K. Sølna, *Wave Propagation and Time Reversal in Randomly Layered Media*, Springer, New York, 2007.
[7] J. Garnier and K. Sølna, Coupled paraxial wave equations in random media in the white-noise regime, *Ann. Appl. Probab.*, **19** (2009), 318-346.
[8] J. Garnier and K. Sølna, Fourth-moment analysis for beam propagation in the white-noise paraxial regime, *Arch. Rational Mech. Anal.*, **220** (2016), 37-81.
[9] J. Garnier and K. Sølna, Paraxial coupling of electromagnetic waves in random media, *SIAM Multiscale Model. Simul.*, **7** (2009), 1928-1955.
[10] J. Garnier and K. Sølna, Imaging through a scattering medium by speckle intensity correlations, *Inverse Problems*, **34** (2018), 094003.
[11] J. Garnier and K. Sølna, Scintillation of partially coherent light in time varying complex media, *J. Opt. Soc. Am. A*, **39** (2022), 1309-1322.
[12] A. Ishimaru, S. Jaruwatanadilok and Y. Kuga, Time reversal effects in random scattering media on superresolution, shower curtain effects, and backscattering enhancement, *Radio Science*, **42** (2007), 1-9.
[13] S. Jaruwatanadilok, A. Ishimaru and Y. Kuga, Optical imaging through clouds and fog, *IEEE Trans. on Geoscience and Remote Sensing*, **41** (2003), 1834-1843.
[14] Y. Kuga and A. Ishimaru, Modulation transfer function of layered inhomogeneous random media using the small-angle approximation, *Appl. Opt.*, **25** (1986), 4382-4385.
[15] X. Pei, H. Shan and X. Xie, Super-resolution imaging with large field of view for distant object through scattering media, *Optics and Lasers in Engineering*, **164** (2023), 107502.
[16] J. W. Strohbehn, (ed.), *Laser Beam Propagation in the Atmosphere*, Springer, Berlin, 1978.
[17] V. I. Tatarskii, *The Effects of the Turbulent Atmosphere on Wave Propagation*, National Technical Information Office, U.S. Dept. of Commerce: Springfield, VA (1971).
[18] L. Thrane, H. T. Yura and P. E. Andersen, Optical coherence tomography: New analytical model and the shower curtain effect, *Proc. SPIE*, **4001** (2000), 202-208.
[19] L. Thrane, H. T. Yura and P. E. Andersen, Analysis of optical coherence tomography systems based on the extended Huygens-Fresnel principle, *J. Opt. Soc. Am. A*, **17** (2000), 484-490.
[20] G. Tremblay, R. Bernier and G. Roy, The shower curtain effect paradoxes, *Proc. SPIE 9641*, Optics in Atmospheric Propagation and Adaptive Systems XVIII, 964107 (2015).
[21] X. Xie, Q. He, Y. Liu, H. Liang and J. Y. Zhou, Non-invasive optical imaging using the extension of the Fourier-domain shower-curtain effect, *Opt. Lett.*, **46** (2021), 98-101.
[22] M. Y. Yahara, Stochastic evolution equations and white noise analysis, *Carleton Mathematical Lecture Notes*, **42**, Carleton Univ., Ottawa, Canada, (1982), 1-80.

Received July 2023; revised January 2024; early access February 2024.